

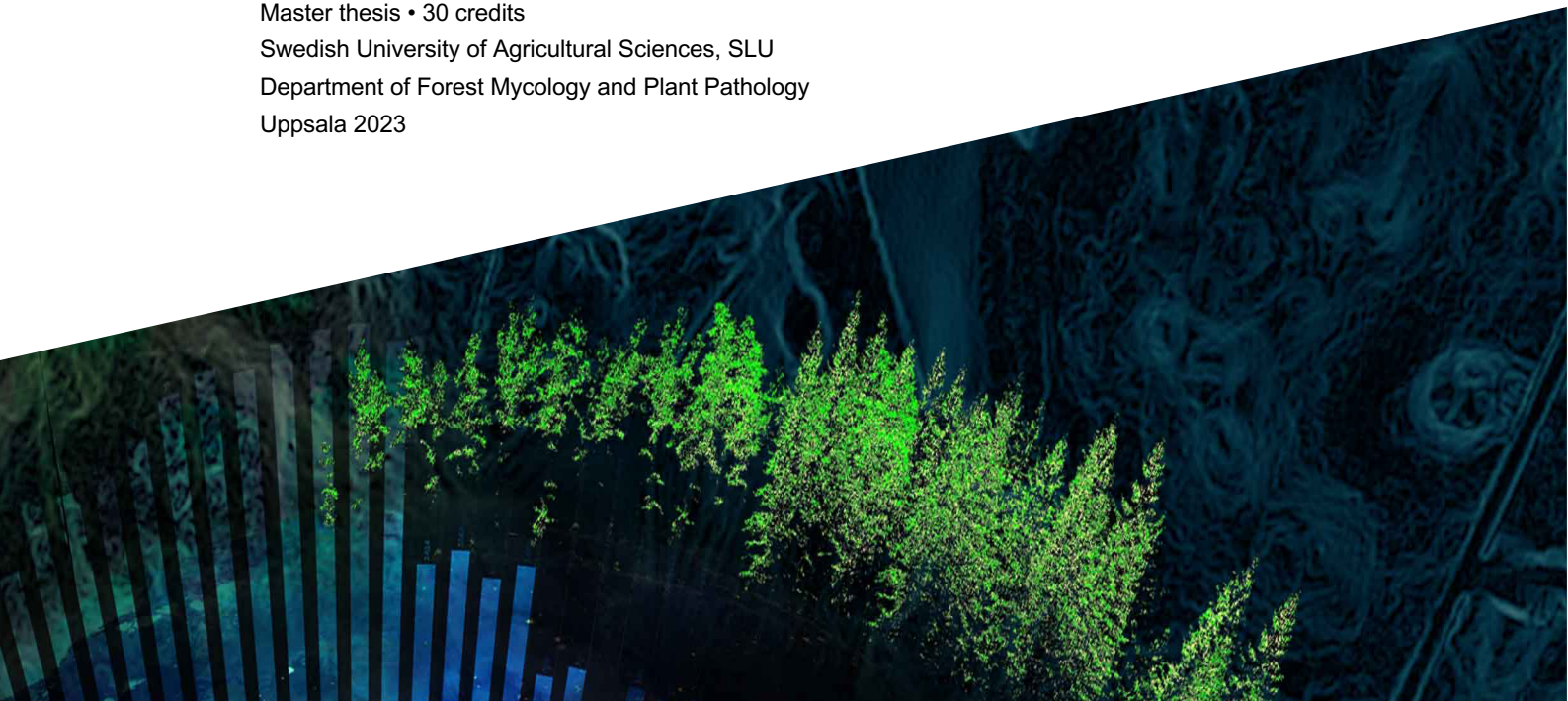


Drought resistance of Ectomycorrhizal fungi in the *Suillus* genus

Torkaresistens hos ektomykorrhizasvampar i
släktet *Suillus*

Patricia Salén

Master thesis • 30 credits
Swedish University of Agricultural Sciences, SLU
Department of Forest Mycology and Plant Pathology
Uppsala 2023



Drought resistance of ectomycorrhizal fungi in the *Suillus* genus

Torkaresistens hos ektomykorrhiza svampar i släktet Suillus.

Patricia Salén

Supervisor: Judith Lundberg-Felten, Swedish University of Agricultural Sciences, Department of Forest Mycology and Plant Pathology

Assistant supervisor: Marisol Sanchez-Garcia, Swedish University of Agricultural Sciences, Department of Forest Mycology and Plant Pathology

Examiner: Anders Dahlberg, Swedish University of Agricultural Sciences, Department of Forest Mycology and Plant Pathology

Credits: 30

Level: A2E

Course title: Master's thesis in biology

Course code: EX0895

Place of publication: Uppsala

Year of publication: 2024

Copyright: All featured images are used with permission from the copyright owner.

Keywords: Ectomycorrhiza, drought, *Suillus*

Swedish University of Agricultural Sciences

Faculty of Forest Sciences

Department of Forest Mycology and Plant Pathology

Unit Forest Microbiology

Abstract

Rising instances of drought are causing more tree seedling fatalities post-nursery outplanting. In the face of climate change, fostering resilient forestry practices is imperative for preserving the health and functionality of our forests. Ectomycorrhizal fungi (ECM), crucial for the drought resistance of key Swedish trees like pine and spruce, play a significant role in forest resilience. With the hypothesis that ECM species with a higher innate drought resistance can more effectively aid their tree symbionts in conditions of drought, it becomes interesting to investigate how drought influences the ECM mycobiont. Differential expressions of specialised water channel proteins called aquaporins (AQPs) have been found under conditions of drought, suggesting an integral role in the drought resilience of ECMs themselves, as well as in the mycorrhizal partnership.

This master project aimed to deepen the understanding of drought resistance in the ectomycorrhizal *Suillus* genus. The characteristics of the gene repertoire of aquaporins within the *Suillus* genus were explored and drought effects on the growth patterns of three fungal species, *S. variegatus*, *S. luteus* and *S. bovinus*, were investigated.

Fungal growth was studied under drought as simulated on Petri dishes by incorporating polyethylene glycol into the agar medium. Only a single isolate, being *S. variegatus* LV-1, showed a significant decrease in diameter and weight when subjected to drought compared to control conditions without PEG. Increased pigmentation and hyphal density were observed across all isolates growing in drought conditions, leading to the conclusion that although drought was achieved, the stress of the mycelium was not generally expressed in terms of diameter of growth or weight. Furthermore, a phylogenetic analysis of AQPs was carried out using the programs MAFFT and FigTree and key amino-acid motifs (i.e. NPA) that influence AQP substrate specificity as well as the topology of *Suillus* AQPs was analysed. Motifs and protein topology in the *Suillus* genus were generally consistent with the literature on fungal AQPs, with a few interesting divergences regarding the NPA motif. The thesis study resulted in the design of primers and validation of stable reference genes for future qPCR analysis of AQPs in *S. variegatus*.

Keywords: Ectomycorrhiza, drought, *Suillus*

Sammanfattning

En ökad förekomst av torka leder till fler dödsfall hos unga träd vid utplantering. I och med klimatförändringarna är det kritiskt att främja hårdigt och beständigt skogsbruk för att bevara hälsan och funktionaliteten av våra skogar. Ektomykorrhizasvampar (ECM) är avgörande för torkaresistensen hos centrala svenska träd såsom tall och gran, och spelar en betydande roll i skogens hållfasthet. Med hypotesen att ECM-arter med en högre torktålighet kan hjälpa sina träd symbionter mer effektivt under torkaförhållanden, blir det intressant att undersöka hur torka påverkar ECM-mykobionten. Differentiella uttryck av specialiserade vattenkanalproteiner, så kallade aquaporiner, har påvisats under torkförhållanden, vilket tyder på att de har en väsentlig roll i ECMs egna torktålighet, samt i den mykorrhizala symbiosen.

Detta masterprojekt syftade till att fördjupa förståelsen för torkaresistensen inom ektomykorrhizasläktet *Suillus*. Genupsättningen av aquaporiner inom *Suillus*-släktet utforskades, och torkans effekter på tillväxten av mycelet av de tre svamparter, *S. variegatus*, *S. luteus* och *S. bovinus*, undersöktes.

Mycelets tillväxt studerades vid torka som simulerades i Petriskålar genom att inkorporera polyetylenglykol i agarmediet. Endast ett enskilt isolat, *S. variegatus* LV-1, visade en signifikant minskning i diameter och vikt när den utsattes för torka jämfört med kontrollförhållanden. Däremot observerades en ökad pigmentering och hyftäthet hos samtliga isolat som växte under torkförhållanden, vilket ledde till slutsatsen att även om torka uppnåddes, uttrycktes inte stressen hos myceliet generellt sett i termer av minskad tillväxtdiameter eller vikt. Därtill genomfördes en fylogenetisk analys av svamp-aquaporiner med hjälp av programmen MAFFT och FigTree. Centrala aminosyramotiv (d.v.s. NPA) som påverkar substratspecificiteten hos aquaporinerna samt topologin hos *Suillus* AQPs analyserades. Aminosyramotiv och proteintopologin hos *Suillus*-släktet var generellt konsekvent med det som hittades i litteraturen angående svamp-aquaporiner, med några intressanta avvikelser gällande NPA-motivet. Examensarbetet resulterade i en framgångsrik design av primrar och validering av stabila referensgener för framtida qPCR-analys av *S. variegatus* aquaporiner

Nyckelord: Ectomycorrhiza, torka, *Suillus*

Table of Content

List of tables	7
List of figures	8
Abbreviations	10
1. Introduction	11
1.1 <i>Aims and Relevance</i>	11
1.1.1 Project Aim	12
2. Background	13
2.1 <i>Ectomycorrhizas (ECM)</i>	13
2.2 <i>Ectomycorrhiza and the forest industry</i>	13
2.3 <i>Drought characteristics</i>	14
2.4 <i>Drought effects on plants and ectomycorrhizal symbionts</i>	15
2.4.1 Aquaporins (AQPs)	17
2.5 <i>The Suillus genus</i>	21
2.6 <i>Hypotheses</i>	21
3. Materials and methodology	23
3.1 <i>Bioinformatics</i>	23
3.1.1 Multiple Sequence Alignment and Phylogeny	23
3.1.2 Aquaporin 3D model prediction	24
3.2 <i>Fungal growth trial</i>	24
3.2.1 Biological Material	24
3.2.2 Qualitative photographic analysis of drought treatment	26
3.3 <i>Reference gene expression analysis</i>	27
3.3.1 Harvest and grinding	27
3.3.2 RNA extraction	28
3.3.3 RNA quantification	28
3.3.4 RNA quality analysis by gel-electrophoresis	28
3.3.5 Primer Design	29
3.3.6 cDNA synthesis	29
3.3.7 Primer Specificity Test by conventional PCR and gel-electrophoresis	30
3.3.8 Primer Efficiency Test by qPCR	30
3.3.9 Reference gene stability analysis by quantitative PCR	31
4. Results	32
4.1 <i>Phylogenetic analysis of AQPs</i>	32
4.1.1 Aquaporin topology	35
4.2 <i>Fungal growth trial</i>	38
4.2.1 Water potential	38
4.2.2 Measured growth	39
4.2.3 Qualitative photographic analysis of drought treatment	40
4.3 <i>Reference gene expression analysis</i>	44
4.3.1 RNA quality analysis by gel-electrophoresis	44

4.3.2	Primer Specificity	44
4.3.3	Primer Efficiency	45
4.3.4	Reference gene expression and stability	47
5.	Discussion	49
5.1	<i>AQP repertoire in the Suillus genus</i>	49
5.2	<i>Technical improvements for growth study</i>	51
5.3	<i>How does drought stress influence Suillus mycelium growth?</i>	52
5.4	<i>Identification of reference genes of Suillus variegatus</i>	54
5.5	<i>Conclusions</i>	55
6.	Future Outlook	56
	References	57
	Popular science summary	64
	Acknowledgements	65
	Appendix	66
6.1	<i>Appendix A – Phylogenetic tree of Dataset 1</i>	66
6.2	<i>Appendix B – Sequence categorisation</i>	67

List of tables

Table 1. Summary of the common NPA variations in loops B and E for each of the clusters, according to literature (Nehls and Dietz, 2014).	21
Table 2. Fungal isolates used in the present study.	25
Table 3. Primer sequences of each reference gene.	29
Table 4. Proteins that have been excluded from the dataset 1. Dataset 1 was used to build dataset 2. Thus, exclusions were made in both datasets unless otherwise specified.	34
Table 5. Cluster, group, and protein ID describes the protein that was used for the model search. The model template describes the protein used in the automated comparative modeling. The GMQE is the Global model evaluation value which describes the overall model quality measurement from 0 and 1 (1 indicating the highest expected quality). Motifs in the NPA-positions shows the motifs that are present in the two (aligned) positions, in loops B and E respectively, that usually contain the NTP motif according to literature.	36
Table 6. Summary of the most important findings from the phylogenetic analysis of AQPs in the <i>Suillus</i> genus.	38
Table 7. Water activity and water potential analysis of PEG treatment conditions.	39
Table 8. Post-hoc Tukey Honestly Significant Difference results for the growth diameters of <i>S. variegatus</i> isolate LV1.	40
Table 9. Post-hoc Tukey Honestly Significant Difference results for the harvest weights of <i>S. variegatus</i> isolate LV1.	40
Table 10. Results from the Directionality test in Fiji on the 80-times magnified stereomicroscopic images of the <i>S. variegatus</i> LV1 and K19 samples treated at 0%- and 20% PEG. The Goodness reports the goodness of the gaussian fit of the histograms. Goodness above 0.5 are marked in green, and bellow 0.5 are marked in orange.	43
Table 11. Primer efficiency summarized from the qPCR results.	47
Table 12. Remarks of the termini of each cluster found in the present study compared to what is reported by Xu et al. (Xu, Cooke and Zwiazek, 2013a).	50
Table 13. Sequences in Cluster I grouped according to 100% identity on both protein- and transcript level.	67
Table 14. Sequences in Cluster II grouped according to 100% identity on both protein- and transcript level.	68
Table 15. Sequences in Cluster III grouped according to 100% identity on both protein- and transcript level.	69

List of figures

Figure 1. Topology of the human aquaporin-1 according to Kruse et al. and Jiang et al. (Kruse, Uehlein and Kaldenhoff, 2006; Jiang, 2009). Figure made in PowerPoint (Version 16.80).	18
Figure 2. An example of how the images were cropped at three places in squares of 2.25 mm ² close to the outer edges of the hyphae. Photo specifically shows the <i>S. variegatus</i> Kat19 0% PEG sample A.	27
Figure 3. Phylogenetic tree of the aquaporins (AQPs) from the three <i>Suillus</i> species (<i>S. variegatus</i> , <i>S. luteus</i> , <i>S. bovinus</i>) of Dataset 2 with clustal categorisation (Cluster I: Orthodox AQPs, Cluster II: Aquaglyceroporins, Cluster III: Facultative AQPs). Made with FigTree... 33	33
Figure 4. a) Number of aquaporin sequences of each cluster per species. b) Number of unique aquaporin sequences (groups) of each cluster per species.	35
Figure 5 Topology of each group in (a) Cluster I, (b) Cluster II, (c) Cluster III. The representative proteins are examples of the proteins in each group. The NPA position column describes the amino acid position of any NPA motifs (N/A for the groups with no NPA motifs). The x-axis of the topological images shows the number of amino acids.	36
Figure 6. a) Model of Suilu4_2769289 from Cluster I, group 1 shown with cytoplasmic side at the bottom, and extracellular at the top of the image. b) Model of Suibov1_1220003 from Cluster II, group 8 shown with cytoplasmic side at the bottom, and extracellular at the top of the image. c) Model of Suibov1_1128812 from Cluster III, group 20 shown from extracellular perspective. Shown in Magneta (red arrows) are the (a) 89NPN and 201NTA, (b) NPA and 236NTA, (c) NPA and 250NPT motifs.	37
Figure 7. Boxplot of (a), (c) the growth diameter and (b), (d) the weights at harvest of the (a) (b) <i>S. variegatus</i> isolates and (b) (c) <i>S. luteus</i> isolates after four weeks of growth. NS is written for the isolates within which no significant difference in growth/diameter was found by the Tukey Honestly Significant Difference test. Unique letters above the bars of the LV1 isolate in a) and b) refer to significant difference (Two-factor ANOVA and Tukey HSD with $p < 0.05$).	40
Figure 8. 0% and 20% PEG samples of the isolates (a, b) <i>S. variegatus</i> Kat19, (c, d) <i>S. variegatus</i> KM1, (e, f) <i>S. variegatus</i> LV1 and (g, h) K5. Photos taken from the bottom of the petri-dishes after four weeks of growth. Growth segmentation is indicated by red arrows in image b), although it is visible in all pictures.	41
Figure 9. Plates of a) <i>S. variegatus</i> KM1 and b) <i>S. bovinus</i> LD2 from first batch of cultivation. Mycelium at one week of growth. Left in image is the 0% PEG plates, and on the right is the 20% PEG plates.	42

Figure 10. Stereomicroscopic images at 80-times magnification. (a, c) 0% PEG condition and (b, d) 20% PEG conditions of the isolates (a, b) <i>S. variegatus</i> Kat19 and (c, d) <i>S. variegatus</i> LV1. Grayscale 8-bit images with scalebar.	42
Figure 11. Results of RNA quality analysis by gel-electrophoresis.	44
Figure 12. Results of primer specificity analysis by gel-electrophoresis. (H1/2 – Histone primer pair 1 and 2, A1/2 Actin primer pair 1 and 2, T1/2 - Tubulin primer pair 1 and 2, U1/2 - Ubiquitin primer pair 1 and 2, P1/2 - Proteasome primer pair 1 and 2).....	45
Figures 13. (a, c, e, g, i, k) Melt Peaks and (b, d, f, h, j, l) Standard Curves for of the primers (a, b) Ubiq1, (c, d) Tub1, (e, f) Tub2, (g, h) His1, (i, j) Act1 and (k, l) Prot1.....	46
Figure 14. Boxplot visualizing the gene expression by the Cq means of the technical replicate. Made in http://shiny.chemgrid.org/boxplotr/	47
Figure 15. Column graph showing the Cq Mean values of each isolate and condition within the six primers as well as the standard deviations of the biological replicates.....	48
Figure 16. Gene stability results produced with the two methods normFinder (left) and Genorm (right) in the web-based PCR analysis program RefFinder (Vandesompele et al., 2002; Andersen, Jensen and Ørntoft, 2004).....	48

Abbreviations

AQP	Aquaporins
ECM	Ectomycorrhiza
PEG	Polyethylene glycol
TMD	Transmembrane domain
XIP	X-intrinsic protein

1. Introduction

1.1 Aims and Relevance

Climate change is an all more undeniable reality. Heatwaves and drought periods are a growing trend, and extreme temperatures are being recorded globally (Guerreiro *et al.*, 2018). Increasing drought periods in summers are leading to higher numbers of tree seedling deaths after outplanting from nurseries. Thus, one of the concomitant issues of the increase of droughts is the effects on renewable resources such as forests (Bailey, Elliott and Schliep, 2021; Lalor *et al.*, 2023; Luoranen, Riikonen and Saksa, 2023). Beyond their roles as environmental regulators and carbon sequesters, forests provide a large array of resources such as fuel, lumber, paper, as well as a variety of foods (Aju, Iwuchukwu and Ibe, 2015). Furthermore, the forest industry is one of the most important business sectors in Sweden (*Swedish forest industry significance*, 2016). With the strain of climate change, resilient forestry is imperative to preserve the forests' functional integrity.

Ectomycorrhizal fungi are natural symbiotic partners to trees such as pine and spruce (Korkama, Pakkanen and Pennanen, 2006), which make up a large majority of the Swedish forest reserve (The Swedish Forest Industries Federation, 2019). Out of the 70 % of Sweden's land area that is composed of forests, 40 % comprises spruce wood, and 39 % pine (The Swedish Forest Industries Federation, 2019). Ectomycorrhizal fungi are important for tree and soil health and the fruiting bodies of the many edible ectomycorrhizal species are appreciated as a food resource (Pérez-Moreno *et al.*, 2021). Ectomycorrhizal fungi can affect drought resistance of trees through various mechanisms. The mycelium network explores wider areas of the soil and can therefore extract additional water. The fungi can also improve nitrogen acquisition and thereby nitrogen use efficiency that requires water uptake. Finally, water transportation to the roots of the hosts can be affected through differential expression of water channels called aquaporins, present in both the tree and the fungus (Lehto and Zwiazek, 2011). While these mechanisms have been observed in a few tree-fungal relationships, it is uncertain today how general they are, which species are best used to improve tree seedlings resistance to drought and whether all ectomycorrhizal fungi provide comparable benefits during drought. Furthermore, we do not know whether a fungus' own drought resistance matters for increasing drought resistance in host trees. If drought resilience of seedlings in nurseries is to be enhanced by ectomycorrhizal inoculation, more knowledge is therefore required to choose appropriate ectomycorrhizal fungi. In extension, knowledge about differences in drought resilience of the ectomycorrhizal species themselves become important. The present study has contributed to the understanding of differential drought resilience among selected ectomycorrhizal species, as this may become crucial for selecting the most effective fungi for enhancing tree seedling survival in nurseries.

1.1.1 Project Aim

This degree project aims to lay a foundation for the understanding of drought resistance in a few species within the ectomycorrhizal fungal genus *Suillus*, which are abundant in forests and easily cultured in the lab. Furthermore, the genome sequence for different species in this genus are available, which allows gene repertoire analysis and facilitates gene expression studies. The ambition is to facilitate future endeavours of understanding and optimising drought resistance of trees with ectomycorrhizal symbiotic relationships.

The main objective of this degree project is to investigate how three species of ectomycorrhizal fungi, *Suillus variegatus*, *Suillus luteus* and *Suillus bovinus* react in conditions of drought. Based on this objective, the following three research questions will be investigated:

- What are the characteristics of the gene repertoire of aquaporins within the *Suillus* genus, and what is the nature and extent of their divergence within and beyond the genus?
- How does simulated drought stress affect the growth patterns of the fungal species?
- How does drought influence the gene expression profile of aquaporins, and what implications does this have for understanding the adaptive strategies for drought tolerance?

2. Background

2.1 Ectomycorrhizas (ECM)

Hyphae are tubular filaments of fungi that build up netlike structures in the soil called mycelium. From a spore or an inoculum, the mycelium grows outwards isotropically, from which the hypha branches by apical expansion. Through hyphal fusion, these branches may interconnect again, producing a network structure (Islam et al., 2017). Many fungi live in symbiosis with plants, an association termed mycorrhiza. In fact, 90 percent of plant species are mycorrhizal. Most mycorrhizal relationships are mutualistic, where the mycelium gets access to the photosynthetically derived carbon produced by the plants, and in exchange supplies the roots with nutrients and water. Mycorrhizae are commonly classified into endomycorrhiza and ectomycorrhiza (ECM). The hyphae of endomycorrhizae penetrate the root cells to establish symbiotic structures (arbuscules), whilst the ECM hyphae surround (but do not penetrate into) epidermal or cortical root cells in an extracellular manner (Bonfante and Anca, 2009). Between 5000 to 6000 species of fungi have been estimated to form ECMs (Molina, Massicotte and Trappe, 1992). The predominant mycobionts in ECMs are the fruiting-body producing basidiomycetes, which mainly create symbiotic relationships with higher plant orders of forest trees such as fir trees or with shrubs (Balestrini and Kottke, 2016) (Smith *et al.*, 2010). The ECM structure consists of the Hartig net, a sheath (mantle) and the extending hyphal network into the soil (extraradical hyphae). The Hartig net is the labyrinthine network of hyphae that grows in between and around the root cells. Covering the root tips, lies the tight mantle or sheath of fungal tissue from which the extraradical mycelium extends (Smith and Read, 2008), (Bonfante and Anca, 2009). The surrounding soil of the root, the so called rhizosphere, contains a third symbiont to the mycorrhizal association, bacteria which may help support the mycorrhizal establishment (Bonfante and Anca, 2009).

2.2 Ectomycorrhiza and the forest industry

Tree-seedling inoculation of ECM fungi is an old practice, dating back to the early 19th century when truffles began to be inoculated with oak seedlings in France. The practice was refined in the mid-20th century, when attempts were made to introduce pines south of the equator. Today, it is recognised that mycorrhizal inoculation of seedlings is imperative to their survival post outplanting in most cases, especially if the soil at the outplanting site lacks suitable fungi. Mycorrhizal deficiencies can be found in soils of agronomic use, in fallowing and denuded soils, or where overcropping or extensive growth of endomycorrhizal trees has been carried out. Furthermore, new nurseries are often set up on lands that have not hosted ECM plants in a long time. The integration of establishing and maintaining healthy

populations of suitable mycorrhizal fungi is a fundamental aspect of effective nursery management (Trappe, 1977).

In the natural environment, the mycorrhizal ecosystems are dynamic, highly complex, and include a large diversity in the fungal symbionts. It is difficult to recreate such an intricate ecosystem, and thus, the outcome of artificial inoculation can differ greatly. Gaining a more comprehensive understanding of the mycorrhizal systems specific to each nursery, type of tree, and site of outplanting is crucial for identifying the most effective inoculation techniques (Cram, Frank and Mallams, 2012). While any form of fungal inoculation is preferable to none, tree nurseries typically employ only a very narrow range of the extensive variety of ECM fungi that exist in nature. Moreover, some ECM fungi species offer greater benefits compared to others, including those species that occur naturally in specific areas. Therefore, it is important to identify which species may be more beneficial for tree survival and growth under specific conditions (Cordell and Omdal, 1990). Specifically, there is limited understanding of how ECM can support tree seedlings in drought conditions and which ECM species are most suited to do so (Castaño *et al.*, 2023).

2.3 Drought characteristics

In natural conditions, lack of water availability for an ECM can occur through drought, high salinity (low external water potential) as well as freezing conditions. Plant responses to low water availability can include growth arrest, membrane damage, protein denaturation, turgor loss, and changes in solute concentrations (Smith *et al.*, 2010). ‘Drought’ refers to the water status, where water is at a lower free energy state than at unstressed conditions. This energy state is quantified as water potential, Ψ_w . Water potential is approximated by two major components, the concentration of dissolved solutes, which describes the osmotic potential Ψ_s , and pressure Ψ_p (Juenger and Verslues, 2023). The water potential can be easily obtained by measuring the water activity with a water activity meter and converting the results to water potential via the relationship in equation 1,

$$\Psi = \frac{RT}{V_m} \ln a_w \quad \text{Equation 1}$$

Where the gas constant, R, is $0.08205 \text{ dm}^3 \text{ atm K}^{-1} \text{ mol}^{-1}$, and the molar volume of water, V_m , is $0.018 \text{ dm}^3 \text{ mol}^{-1}$ (Adams, Moss and McClure, 2016).

When simulating drought, it is important to determine the Ψ_w at which the experiment is being conducted, as this describes the severity of the drought in a manner which can be replicated across experimental systems (Juenger and Verslues, 2023). A Ψ_w of $<-0.8 \text{ MPa}$ is generally recognised as an indication of drought stress (Osmolovskaya *et al.*, 2018). The importance of determining the Ψ_w of an experimental condition can be highlighted by looking at the relationship between soil water content versus Ψ_w . In soils of smaller particle size (such as clay), there needs to be much more water content to obtain the same Ψ_w as in soils with larger particles. This is due to the effects of water adhesion on the available surface area of the particles (Juenger and Verslues, 2023). However, other effects of drought should also be pondered. With a lower water content, there is increased nutrient concentration. Furthermore, drought also leads to changes in the soil structure, and the rhizosphere microbiome as well as higher vapor pressure deficit, all of which may have compounding effects on the mycorrhiza in bona-fide drought (Gonzalez *et al.*, 2022). For example, at a lower Ψ_w in soil, there is also a decline in the soil hydraulic conductivity. This means that the remaining water molecules are

more tightly bound to the soil and regulate how much water is available to the mycorrhizal components (Juenger and Verslues, 2023).

To investigate responses to drought at physiological and molecular levels, it is important to mimic authentic drought conditions. This can, however, become quite challenging (Gonzalez *et al.*, 2022). There are three general categories of experimental drought simulation, each with its own limitations. These categories are soil-, aqueous culture- and agar-based setups. Although soil-based investigations have a close similarity to natural drought conditions, they entail challenges such as difficulty in extracting intact root systems, in quantifying evaporation from the soil, and to control the Ψ_w . Reproducibility and predictability of soil-based drought simulation is generally thought to be questionable. Hydroponic aqueous cultures have been used for drought simulation by supplementation with osmotically active substances that reduce the water availability. These osmolyte substances thereby simulate drought by applying osmotic stress through increase of the medium osmotic pressure. This imitates natural drought where the decrease of water content in the soil entails an increase of solute concentration. However, as osmolytes can have strong negative side effects, the selection of appropriate osmolytes is imperative. The method of choice of drought stress simulation in molecular biology is currently the application of polyethylene glycol (PEG), which is presumed to be inert and non-permeable (Osmolovskaya *et al.*, 2018). PEG, which is of high molecular weight, has been deemed to cause a condition more similar to drought than osmotic stress that is imposed by low molecular weight solutes. This is because PEG reduces Ψ_w by matric forces rather than osmotic forces. Some of the limitations of PEG-based conditions relate to the high viscosity of this high molecular weight compound. The high viscosity compromises the oxygen diffusion in the media, which can cause hypoxia. The hypoxic state can be reduced or avoided by growth in agar. A combined method of agar-based PEG infusion is therefore deemed favourable. As PEG affects the solidification of agar, it is advised to use a model where PEG is allowed to diffuse into solidified agar in Petri dishes from a PEG-containing medium overlay. The concentration of PEG in the overlay adjusts the Ψ_w equilibrium between the layers within 24 h of diffusion. After equilibrium is assumed to be reached, the overlay can be decanted, and the now PEG-containing agar can be inoculated with the ECM fungi. This PEG-agar model is deemed ideal due to its reproducible and stable nature. However, it is important to note that due to its simplicity, the model does not allow direct extrapolation of natural drought effects (Osmolovskaya *et al.*, 2018). Furthermore, possible absorption and accumulation of PEG might result in cell damage. Although a study by Yaniv and Werker (Yaniv and Werker, 1983) showed that PEG was secreted from leaves of plants exposed to PEG-based water stress, it is today still generally assumed to be an inert non-penetrative substance by many studies (Abbas *et al.*, 2014; Piwowarczyk, Kamińska and Rybiński, 2014; Imtiaz *et al.*, 2020; Khalid, Kumari and Nasim, 2021; Mahpara *et al.*, 2022). It merits attention that no studies could be found where the described method using a PEG overlay solution on solid agar medium has been used on mycelial fungi.

2.4 Drought effects on plants and ectomycorrhizal symbionts

Drought is one of the most prevalent environmental stressors of plants and adversely impacts their development, growth, and reproduction. Drought impacts plants to varying degrees depending on the developmental stage of the plant itself as well as the duration and intensity of the drought. Drought not only leads to less water uptake by the roots, but also to a lower nutrient uptake due to the decrease of nutrient diffusion and mass flow in the soil as well as a

lower degree of mineralization of organic matter. This can lead to deficits of nitrogen and phosphorous in the plant (Bista *et al.*, 2018).

In plants, water evaporates through surface pore-structures in the leaves called stomata. The stomata opening allows for carbon dioxide entry as well as water vapor loss. Through the loss of water at the leaves, a lower water potential and negative hydrostatic pressure allows for water uptake at the roots in a process called transpiration (Querejeta, Egerton-Warburton and Allen, 2003). During transpiration, the degree of opening at the stomata regulates the water uptake. But the reverse is also true as the water availability in the soil affects the hydrostatic pressure gradient and the degree of opening at the stomata (the stomatal conductance). This is an important feedback loop for water conservation under conditions of drought (Smith *et al.*, 2010). During water stress, the decreased water uptake leads to a lower degree of leaf expansion and stomatal conductance (Bista *et al.*, 2018). The smaller stomatal aperture limits carbon dioxide influx, which leads to a decline in the rate of photosynthesis (Bacelar *et al.*, 2012). This causes reduced carbon assimilation through photosynthesis (Bista *et al.*, 2018).

Water stress also leads to oxidative stress through an overproduction of reactive oxygen species (ROS). ROS cause damage to lipids, DNA, proteins, and carbohydrates. The oxidative stress, in turn, impairs essential enzymes and ATP synthesis, leading to damage of the photosynthetic and respiratory systems (Bacelar *et al.*, 2012).

The benefit of the mutualistic relationship experienced by the plant symbiont of a mycorrhizal interaction relates to efficient nutrient, mineral and water uptake and use, increased carbon dioxide fixation rates as well as an increased tolerance to stresses (Bonfante and Anca, 2009). As a large majority of land plants are dependent on such an association, there lies great economic and environmental potential in the understanding and exploitation of mycorrhizal systems (Bonfante and Anca, 2009). In fact, ECM mycelia can compose up to 30 percent of the total soil microbial biomass in forests (Dietz *et al.*, 2011).

ECM fungi have multiple strategies to help the plant symbiont in conditions of drought. The most obvious strategy regards the water access of the plant via structural aspects. Through the mycelium network, the roots get access to an 100-1000-times increased interface area of water uptake as the hyphae are significantly smaller than the plant root hairs. Thus, higher efficiency can be achieved for the uptake of immobile nutrients, which in general reduces the need for large-volume water transport as the plants have access to the same amounts of nutrients at a lower water demand. Furthermore, ECM species have been shown to improve the rhizosphere nutrition content by increasing the soil enzyme activity (Yin *et al.*, 2018).

Due to the small size of the hyphae, they have access to pore water between the soil particles, which becomes of particular value in drought. Furthermore, the hyphae are able to absorb water from soils with lower water potentials. Water transportation through mycelium is driven by osmotic potential (Varma, 2008). Some hyphae develop into vessel type strands, rhizomorphs, that are specifically effective for medium- to long-distance exploration of soil (Agerer, 2001). Rhizomorphs have enlarged, modified structures, inter alia with removed septa and thickened cell walls, which assist in fast movement of water with minimal water loss (Xu and Zwiazek, 2020).

In a more qualitative aspect of this mutualistic relationship, the ECM modulates the water requisite of the plant (Smith *et al.*, 2010). It has been shown that mycorrhizal symbiosis leads to a higher water-use efficiency (increased acquisition of nutrients at a lower water demand)

and a lower stomatal resistance, which leads to higher water uptake and carbon dioxide fixation rates. ECM also affects the internal water transport, through both the apoplastic and symplastic pathways, of the plant (Varma, 2008).

Furthermore, mycorrhizae (more research done in endomycorrhiza compared to ECM) have been well documented to enhance the antioxidant activity through enzymes such as CAT, POD, and SOD. Thus, they can decrease the levels of oxidative stress, which conserves some of the photosynthetic and respiratory activities which would otherwise be damaged (Wu, Xia and Zou, 2008; Zhang *et al.*, 2010; Zhu, Song and Xu, 2010; Yin *et al.*, 2018).

During drought, plants can regulate their osmotic potential through accumulation of sugar, free proline, and soluble sugars. A study by Yin *et al.*, found that colonization with a *Suillus* species lead to an increased accumulation of carbohydrates, which in turn reduced the osmotic potential of the host. Further, inoculation of the *Suillus* species also resulted in a lower proline accumulation in the host, indicating improved drought tolerance (Yin *et al.*, 2018).

An interesting actor with potential of contributing to the drought resistance of both the fungi and their hosts, is a water channel protein called Aquaporin (AQP). Studies have shown that the fungal expression of these water transportation proteins increases during conditions of drought, leading to higher rates of water transportation than otherwise possible (Xu and Zwiazek, 2020).

The mycorrhizal association can be beneficial to the plant symbiont to a certain degree, but if the level of soil hydration is too low for even the mycelium to survive, no such benefits are observed. Therefore, it is important to understand the drought sensitivity of the mycelium itself (Varma, 2008). Castaño *et al.* (2023) observed in greenhouse conditions that although short-term drought decreased the amount of mycelia in the soil, the trees that did survive drought had formed more mycorrhizal partnerships with ECM fungi than the well-watered trees. They even noted that some trees with specific mycobionts were even promoted by drought. They concluded that ECM taxa with a higher biomass, and commonly with hydrophobic mantle and rhizomorphs, so called long exploration types (such as *Suillus*), had higher drought resistance as they were better adapted to forage for water (Castaño *et al.*, 2023).

2.4.1 Aquaporins (AQPs)

Although water diffuses through lipid bilayers, lower temperatures entail lowered membrane water permeabilities due to tighter packing of the lipids. Diffusion is enhanced greatly by Major Intrinsic Proteins (MIPs) also called aquaporins (Dietz *et al.*, 2011). AQPs are gradient-driven transmembrane proteins that transport, to different degrees, uncharged molecules such as water, urea, glycerol, ammonia, carbon dioxide etc. (Smith *et al.*, 2010; Dietz *et al.*, 2011; Xu and Zwiazek, 2020). Although AQPs are present in all kingdoms, the gene families of the fungal AQPs are considerably smaller than those of animals and plants and only a few AQPs have been functionally characterised (Nehls and Dietz, 2014).

Aquaporins generally consist of 250-330 amino acids arranged into six helical transmembrane domains jointly forming an hourglass-like channel (Nehls and Dietz, 2014; Xu and Zwiazek, 2020). Helices 1-3 are imperfect repeats of the opposite orientation to helices 4-6. Out of the five loops between these domains, three are located extracellularly, and two loops and two termini intercellularly, as visualised in Figure 1. The N-terminus motifs predicts the subcellular

localization of the AQP on the plasma membrane, secretory pathway or mitochondrial membrane (Xu and Zwiazek, 2020). Furthermore, the AQP surface is coated with hydrophobic residues, which prevents protein-water interactions. AQPs can construct homo- and heterotetramers, the monomeric composition affects the overall pattern of permeability (Nehls and Dietz, 2014).

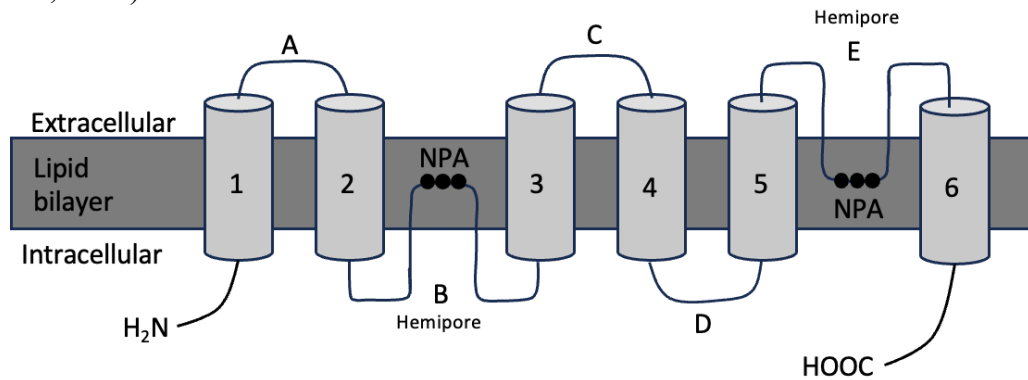


Figure 1. Topology of the human aquaporin-1 according to Kruse *et al.* and Jiang *et al.* (Kruse, Uehlein and Kaldenhoff, 2006; Jiang, 2009). Figure made in PowerPoint (Version 16.80).

The AQP selectivity is determined by the electrostatic properties, the hydrophobicity, and the diameter of the channel (Nehls and Dietz, 2014). The smallest section of the pore consists of highly conserved arginine and aromatic residues and acts as a selectivity filter, preventing protons from passing. This ar/R filter consists of histidine residues from the second and fifth transmembrane domains as well as two residues from the first and second loops. A second factor affecting the selectivity are so-called Froger positions, which contain highly conserved amino acids that discriminate between glycerol and water (Li *et al.*, 2021). The selectivity is also affected by two of the loops (the second and fifth loop) which are hydrophobic with short alpha-helices which fold into the monomer in the membrane. Thus, the helices position two asparagine-proline-alanine (NPA) signature motifs into the channel's centre. These highly conserved NPA motifs are found in almost all AQPs and are found to be important for structure and function of the AQP (Jiang, 2009; Nehls and Dietz, 2014). A positive electrostatic field is created in the aqueous lumen due to the N-termini of the helices which are directed into the centre. The electrostatic field orients the oxygen atoms of the water molecules towards the asparagine residues of the NPA, between which hydrogen bonds are formed. A single file of water transported through the AQP is the effect of the making and breaking of two of these hydrogen bonds. By the breaking of the bond, the water molecule switches direction, which prevents 'proton networks' to form. The positively charged His74 and Arg195 of either loop are highly conserved and prevent ions from passing through the pore. The high speed in which water passes through the pore is facilitated by hydrophobic nature of in the channel with only a few hydrophilic nodes (the Ala73, His74 node, the Asn76, Asn192 node of the NPA motif, and the His180, Gly190 node) which can form hydrogen bonds with four water molecules (Jiang, 2009).

In the hyphae, the AQPs regulate the amount of water entering the mycelial complex and the rhizomorphs. Then, fungal AQPs in the Hartig net impact the water availability at the root extracellular space, which in turn influences the root AQP regulation and root water uptake (Xu and Zwiazek, 2020). The average soil temperature of boreal forests lies between 5-10°C at the compartment where ECMs are commonly found. The low temperatures in combination with the high flux of water can explain the necessity of AQPs (Dietz *et al.*, 2011).

Water movement is influenced by both the number of expressed AQPs and their activity.

AQP expression is hormonally regulated both spatially and developmentally in a cell-specific manner (Marjanović *et al.*, 2005). Environmental stimuli can affect AQP expression and include drought, salt, temperature, pH and mycorrhization (Xu and Zwiazek, 2020).

AQP activity is regulated on the protein level by posttranslational modifications such as phosphorylation/dephosphorylation of serine residues and on oligomerization (Smith *et al.*, 2010; Aroca and Ruiz-Lozano, 2017). During water stress, some AQPs show lower phosphorylation which reduces activity and can thereby limit water loss (Smith *et al.*, 2010).

2.3.2.1 The AQP gene family in plants and fungi

Based on AQP selectivity deduced from protein sequence (Froger *et al.*, 1998), topology and electrostatic properties of the channel region, they can be distinguished to preferentially transport, at high rates, either only water (called true or orthodox aquaporins), mostly solutes (called aquaglyceroporins) or both water and solutes (bifunctional AQPs) (Gena *et al.*, 2011). This simple classification is contrasted by phylogenetic grouping of AQPs, that even may take into account subcellular localization, physiological function, selectivity and efficiency and can lead to classification of AQPs into up to 30 subfamilies depending on the number and types of organism analysed (Zardoya, 2012). In the following paragraphs, the focus will be on plant and fungal AQPs. (Zardoya, 2012)

AQPs are abundant in both plants and fungi. More than 35 different AQP-like genes have been sequenced in the genome of *Arabidopsis thaliana* alone (Kruse, Uehlein and Kaldenhoff, 2006) and 229 AQPs from 88 fungal species across four phyla of Mycota were included in a phylogenetic analysis by Xu *et al.* (Xu, Cooke and Zwiazek, 2013a). AQPs from plants and fungi have been categorised in different ways. Plant AQPs can be categorised based on their gene sequence, sub-cellular localization, or homology to known proteins (Johanson *et al.*, 2001) into the groups Nodulin-intrinsic proteins (NIPs), Plasma membrane intrinsic proteins (PIPs), Small intrinsic proteins (SIPs), and Tonoplast intrinsic proteins (TIPs) (Chaumont *et al.*, 2001; Ishikawa *et al.*, 2005; Marjanović *et al.*, 2005). The PIP category is especially important for determination of root hydraulic conductivity regulation as well as uptake of water via the roots. Abscisic acid (ABA) is a plant hormone that regulates water deficit plant response and has been reported to induce transcription factors for the expression of PIP AQPs (Groppa, Benavides and Zawoznik, 2012). It has even been suggested that some plants, among them moss and *Populus*, but also fungi contain a fifth AQP cluster, called XIPs (unrecognised X intrinsic proteins), that is more hydrophobic and may transport other solutes (Danielson and Johanson, 2008; Gupta and Sankararamkrishnan, 2009).

Clustering of fungal AQPs is, unlike plant AQP clustering, often less informed by experimental data since both functional analyses or subcellular localization have in most cases not been conducted yet. However, the increasing number of available fungal genomes, including yeast, filamentous and ECM fungi, has made phylogenetic analyses of fungal AQPs possible (Pettersson *et al.*, 2005; Dietz *et al.*, 2011). Such analyses have also been supported by gene expression data. Phylogenetic analysis of fungal AQPs revealed four groups: orthodox AQPs, Fps-like aquaglyceroporins, aquaglyceroporins, and X-intrinsic proteins, XIPs (Dietz *et al.*, 2011). Fps-like AQPs were initially defined as a group of yeast AQPs harbouring a conserved regulatory N-terminal domain specific to yeast (Pettersson *et al.*, 2005). Even though other fungal AQPs may lack this domain, their overall similarity to Fps-like aquaglyceroporins justified their belonging to this group. XIPs comprise the smallest of the fungal AQP groups

and are absent in multiple fungal clades, including the ECM model fungus *Laccaria bicolor* even though they are present in other basidiomycetes (Nehls and Dietz, 2014). The proportion between the AQP groups was investigated by Nehls and Dietz (Nehls and Dietz, 2014). Out of 16 genomes of Boletales (the order to which the genus *Suillus* belongs), they found that a mean number of 1.2 of the AQP in each genome belonged to orthodox AQPs, 2.9 were categorised as XIPs, and 0 were found to belong to the aquaglyceroporin groups (Kretzer and Bruns, 1999; Nehls and Dietz, 2014). However, they also described that only 9.7% of all deduced AQPs in fungal genomes belonged to XIPs. Also, Correia *et al.* found that orthodox AQPs contribute to 41 percent of the deduced fungal AQPs and are commonly found in *Basidiomycota*, the phyla containing the majority of all ECMs (Correia *et al.*, 2021).

An alternative nomenclature and categorization of AQPs which is also based on phylogenetic analysis is found in literature as well: orthodox AQPs can be called Cluster I AQPs, Fps-like aquaglyceroporins and genes belonging to species of *Basidiomycota* and filamentous *Ascomycota* phylum are collectively termed Cluster II, 82 fungal AQPs that are non-monophyletic can be categorised as Cluster III (also called facultative fungal AQPs or Yfl054-like AQPs), and finally, XIPs can be called Cluster IV. Cluster I AQPs have six TMDs in general, with some exceptions which may contain five or seven TMDs (Xu, Cooke and Zwiazek, 2013a). Compared to other organisms, fungal Cluster I AQPs show more variations in both NPA positions, with substitutions in the A or P position (NPX/NXA), see Table 1 (Nehls and Dietz, 2014). In loop B, NPX substitutions are occasionally observed, where alanine (A) has been substituted for threonine (T), valine (V), serine (S), cysteine (C), or asparagine (N), and in loop E, NXA substitutions have been documented (although NPV has also been found), where P has been substituted for phenylalanine (F), S, T, V, or tryptophan (W) (Xu, Cooke and Zwiazek, 2013a). Lacbi1:392091 of *L. bicolor* (*Basidiomycota*) has been found to contain NPN/NSA motifs instead of NPA (Dietz *et al.*, 2011), and GintAQPf1 of *Rhizophagus intraradices* (AMF *Glomeromycota*) has been found to contain NPS/NPA motifs in the protein sequence (Li *et al.*, 2013). The water transport capacity of Cluster I AQPs is particularly noteworthy for exploring the water uptake mediated by fungal AQPs in mycorrhizal plant systems (Xu, Cooke and Zwiazek, 2013a). Cluster II proteins are predicted to have five to seven TMDs and to have long termini. The NPA motif of these sequences has been found to be replaced with SPA or NPC. Alternatively, loop E has been found contain NXA substitutions, where P can be substituted with N, L, S, M, T, or A. Substitutions of these kinds has been hypothesised to be related to the lower water permeability of this group. Cluster II AQPs are, however, predicted to have an increased permeability for glycerol and methylamine. Despite a lower water permeability, the Cluster II AQPs may be important for osmotic adjustment in mycorrhizal-plant symbiosis. Cluster III AQPs generally contain six TMDs, although variations of 5-7 TMDs can be found. Their NPA motif in loops B can be substituted to NPA, NPS, NPV, or NPT, and substituted to NLA, NPA, NGA, NFA, NMA, or NAA in loop E. Lastly, Cluster IV exhibit six TMDs with several variants of the NPA motif in loop B and E, for example NPA/T/L/M, NSM, or SPT can be found. For Cluster IV proteins with seven TMDs, the NPA of the final loop (loop D) is more conserved than for loop B and E (Xu, Cooke and Zwiazek, 2013a).

Table 1. Summary of the common NPA variations in loops B and E for each of the clusters, according to literature (Nehls and Dietz, 2014).

Cluster	Loop B motif	Loop E motif
Cluster I	NPX	NXA
Cluster II	SPA/NPC	NXA
Cluster III	NPX	NXA

2.5 The *Suillus* genus

Fungi of the *Suillus* genus are almost exclusive ectomycorrhizal (ECM) partners with *Pinaceae*, although most ECM fungi are generalists. Due to their host-specificity, *Suillus* are found in the northern hemisphere, predominantly in temperate and boreal forests where *Pinaceae* grow. The genus is heterothallic with a bipolar sexual incompatibility (sexual reproduction only occurs between opposite mating types) (Cairney and Chambers, 1999). The *Suillus* are one of the most prominent fruiting species in pine forests (Cairney and Chambers, 1999), which points to their gastronomic value, as *Suillus* is a typical edible ECM genera (Guevara-Gonzalez and Torres-Pacheco, 2014).

Three species of *Suillus* are investigated in the present study: *S. luteus*, *S. variegatus*, and *S. bovinus*. The latter two are mainly found in dry pine forests where the soils are sandy and acidic and are especially known as mycobionts to Scots pine, *Pinus sylvestris* L. In such dry forests, *S. variegatus* constitutes ca. 25% (but sometimes up to 60%) of the ECM sporocarp biomass, whilst *S. bovinus* only constitutes up to 0.5%. *S. variegatus* is less abundant in younger forests, where *S. bovinus* is more abundant. With the presumption that the number of sporocarps correlates with the mycorrhizal biomass, the gradual displacement of *S. bovinus* by *S. variegatus* with increasing forest age might imply enhanced adaptation of *S. variegatus* to later phases in the progression of forest succession (Dahlberg, 1997). The basidiomycete *S. luteus* grows in heavy metal-polluted soils in younger forests. *S. luteus* usually colonises pine seedlings by way of spores transported with wind or mammals. The generation time of the species is quite short, 3-5 years. Due to its frequent sexual reproduction, genetic adaptation to specific soil conditions is hypothesised to be developed more rapidly (Muller, Vangronsveld and Colpaert, 2007). *S. bovinus* growth pattern differs from that of *S. variegatus*. It grows with smaller populations over a few localities, and can be considered a satellite species, whilst *S. variegatus* can be considered a core species with large populations in most localities of the forest. Furthermore, it has been considered likely that genets of *S. variegatus* persist between generations of forests (Dahlberg, 1997).

2.6 Hypotheses

In literature, it was found that the fungal AQP sequences primarily belonged to clusters I-III, with fewer proteins belonging to the fourth cluster (SOURCE). It was also found that Cluster I AQPs have particular potential for water uptake and that when substitutions are present in the NPA motif of fungal AQPs, NPX substitutions in loop B and/or NXA substitutions in loop E are the commonly observed substitutions. From this, the following hypotheses were postulated for the first research question, What are the characteristics of the gene repertoire of

aquaporins within the *Suillus* genus, and what is the nature and extent of their divergence within and beyond the genus?:

- The three *Suillus* species primarily contain AQPs protein sequences of Cluster I-III, and fewer Cluster IV proteins if any.
- A higher prevalence of Cluster I AQPs are found in species that have higher drought resilience.
- If substitutions of the NPA motif are found, these will be observed to be NPX (loop B) and/or NXA (loop E) substitutions.

The species investigated in the present thesis are *S. variegatus*, *S. luteus*, and *S. bovinus*. It was found in literature that *S. variegatus* and *S. bovinus* are specifically found in dry soils. Further, *S. bovinus* was found to be a satellite species, whilst *S. variegatus* is more broadly spread out. Based on these literary findings, the hypotheses that were tested for the second research question, *How does simulated drought stress affect the growth patterns of the fungal species?*, were the following:

- *S. variegatus* and *S. bovinus* are more drought resilient and therefore show less/milder signs of stress in conditions of drought than *S. luteus*.
- *S. variegatus* is more adaptable and in extension more resilient than the other two species of *Suillus*.
- In general, high drought stress will significantly alter the growth patterns of the fungal species, resulting in reduced mycelial expansion and altered morphology.

Finally, hypotheses for the third research question, *How does drought influence the gene expression profile of aquaporins, and what implications does this have for understanding the adaptive strategies for drought tolerance?*, were inferred based on the literature regarding the relationship between AQP expression and water transportation. These hypotheses were:

- Drought conditions will result in an increase in the expression of aquaporin genes in the *Suillus* species.
- Specifically, Cluster I aquaporin will be expressed to a higher extent during drought relative to the other clusters.

The outcome from the master's thesis study was expected to facilitate the future endeavours of exploring the symbiotic relationship of fungus and host in conditions of drought. A deeper understanding of which fungal species relate to higher drought resilience of the mycelium itself will hopefully also aid in advancement of research related to mycorrhizal drought resilience, and in extension, the drought resistance of plants.

3. Materials and methodology

3.1 Bioinformatics

3.1.1 Multiple Sequence Alignment and Phylogeny

The dataset created for this research was compiled by searching mycorrhizal fungal genomes with the keyword “aquaporin” in the JGI database, specifically at https://mycocosm.jgi.doe.gov/Mycorrhizal_fungi/Mycorrhizal_fungi.info.html. Two outgroups, AQPZ from *Escherichia coli* (Genbank ID: CAD6018024) and AQP1 from *Mus musculus* (Genbank ID: AAH07125) were added to what was then referred to as dataset one (D1). These outgroups were chosen as they have already successfully served as reference AQPs in the study *Phylogenetic analysis of fungal aquaporins provides insight into their possible role in water transport of mycorrhizal associations* (Xu, Cooke and Zwiazek, 2013b). D1 was further extended by blasting each *Suillus* putative AQP protein in the dataset against all model proteins in the genome of the respective three *Suillus* species analysed. For *Suillus bovinus*, the database 20180813 was used (Lofgren *et al.*, 2021), for *Suillus variegatus*, 20180923 was used (Lofgren *et al.*, 2021), and for *Suillus luteus*, 20170628 was used (Kohler *et al.*, 2015). All alignment hits were collected and further analysed. First, the protein topologies of the proteins in the datasets were analysed using both Mycocosm (Grigoriev *et al.*, 2014) and <https://dtu.biolib.com/DeepTMHMM> (Hallgren *et al.*, 2022). As six transmembrane domains are expected for aquaporin proteins according to literature, the proteins that showed four transmembrane domains or fewer were excluded from the datasets. In addition to the protein sequences, the transcripts, and genes of all proteins in the datasets were retrieved. If a protein did not have a transcript or gene sequence uploaded to Mycocosm, it too was excluded from the datasets.

The protein sequences of both datasets were aligned using the programme MAFFT (Kato, 2023). The Fast Fourier Transform strategy with iterative refinement (FFT-NS-2) was used with no additional arguments. To create a phylogenetic tree from the alignment, the programme IQTree was employed. Firstly, an extended model selection followed by tree inference was conducted using the -m MFP command. For D2, a standard nonparametric bootstrap value was set to 100 and the best number of CPU cores was automatically determined based on the current data using the ‘-nt AUTO’ command. For D1, the ultrafast bootstrap with 1000 replicates was instead employed due to time limitations. Finally, the phylogenetic tree was visualised in FigTree (Rambaut, 2007). Outliers were excluded by pruning the tree with R (R Core Team, 2020), using the package ape (Paradis and Schliep, 2019) and the function drop.tip().

The following five proteins were used as references for the respective clusters (clustal signature reference proteins): *Laccaria bicolor* Lacbi2|[456764](#) representing cluster I, Lacbi2|[671860](#)

representing cluster II, Lacbi2|317173 for cluster III and finally, *Tuber melanosporum* TmeAQP2 as reference for cluster IV (Xu, Cooke and Zwiazek, 2013a). The reference proteins were blasted against D1 and D2. The clade organization and percent identity results were then used to infer the cluster categorization within D1 and D2. The cluster categorisation was visualised in the phylogenetic tree.

In each cluster, the proteins were grouped together when two or more sequences were 100% identical on protein sequence level, transcript level. The group contents were compared. The topologies of the proteins were compared across the groups that were identical on both protein and transcript level, and cluster-specific topological characteristics were interpreted. The topologies were analysed using both MycoCosm and DeepTMHMM, an online protein structure prediction application found at <https://dtu.biolib.com/DeepTMHMM> (Nordberg *et al.*, 2014; Hallgren *et al.*, 2022).

3.1.2 Aquaporin 3D model prediction

The positions of NPA motifs and possible substitutions (NPX or NXA substitutions, according to literature (Nehls and Dietz, 2014)) were found in the protein sequences using Aliview (Larsson, 2014). Substitutions were categorised according to species and cluster. At least one sequence per cluster and species was visualised in YASARA (Krieger and Vriend, 2014). For this, the target sequence was pasted in the online modelling tool Swissmodel (<https://swissmodel.expasy.org/>) (Guex, Peitsch and Schwede, 2009; Bertoni *et al.*, 2017; Bienert *et al.*, 2017; Waterhouse *et al.*, 2018; Studer *et al.*, 2020) in FASTA format. An automodel was built and uploaded to YASARA. Any NPA motifs and each of the possible substitution motifs were inspected in the 3D model. The motifs (either NPA or a substitution motif) that were positioned according to the NPA-motifs in literature, i.e. in one of the hydrophobic loops (B- and E- loops, see Figure 1) with short alpha-helices that fold into the monomer were coloured.

3.2 Fungal growth trial

3.2.1 Biological Material

To examine

A total of nine isolates within three species of the genus *Suillus* were used in the present study. Four isolates within the species *Suillus variegatus*, two *Suillus luteus*, and three within *Suillus bovinus*, see **Error! Reference source not found.** These isolates had been previously isolated by other lab members from different areas in Northern and middle Sweden or obtained from a Finnish collaboration partner.

Table 2. Fungal isolates used in the present study.

Species	Name of isolates	Origin
<i>Suillus variegatus</i>	Kat 19	Uppland (Fiby Urskog)
	MMK	Finland
	KM1	Västerbotten (Bureå)
	LV1	Västerbotten (Bureå)
<i>Suillus luteus</i>	Kat 5	Västergötland (Billingen)
	KS1	Västerbotten (Umeå)
<i>Suillus bovinus</i>	Kat 4	Västergötland (Billingen)
	Kat 16	Västergötland (Skövde)
	LD2	Västerbotten (Bureå)

The selected *Suillus* species (see 2.1) were precultured on 1/2 MMN agar (15g/L) solidified media in 9 cm diameter round Petri dishes. They were grown in darkness at 25°C.

½ MMN media was prepared containing 1.25 g/L D+ glucose monohydrate, 5 g/L malt extract, 0.25 g/L diammonium phosphate, 0.5 g/L monopotassium phosphate, 0.15 g/L magnesium sulphate heptahydrate salt, 0.05 g/L calcium chloride dihydrate, 0.025 g/L sodium chloride, 0.02 g/L ferric EDTA, 0.02 g/L thiamine hydrochloride, and 15 g/L agar agar. The pH was adjusted to 5.5 before it was autoclaved. 20 mL media was poured into 9cm round Petri dishes under a hood and sterile conditions. After 10 min of drying, the Petri dishes were closed, and the solidified agar dishes were kept at 4°C under sterile conditions until use.

To investigate the isolates at different levels of osmotic stress PEG was added to the media. The growth experiment was conducted twice, due to contamination of many of the plates in the first batch. The first experiment used a highest drought condition of 20% PEG which was dismissed for the second experiment. This was due to the high density of the PEG, which resulted in release of the agar from the Petri dishes when the PEG overlay solution was decanted. The growth of the first experiment showed clear indications of drought already at 10% PEG. The drought was exhibitive in that the inoculation plugs were increasingly shrivelled in accordance with the drought gradient. Thus, for the second try, the drought gradient was changed to 0%, 5%, 7.5% and 10% PEG. For the second experiment, 4 biological replicates per condition and fungal strain were prepared on 53 mm plates, with four drought conditions (0, 10, 15 and 20 % w/v PEG in overlaid solution).

PEG plates were prepared as follows: A liquid ½ MMN PEG blend was prepared by first making a 10x concentrated media which was autoclaved. As PEG cannot be autoclaved, the pre-weighed amounts were placed under UV light for 20 minutes. Under a sterile bench, 10, 15 and 20 %w/v PEG was dissolved in 1x MMN and the pH was confirmed at 5.5 (no adjustment was required). An equal volume as the previously poured solidified 1/2MMN medium was then poured of the 0, 10, 15, and 20 %w/v PEG solutions onto the solidified agar in pre-prepared Petri dishes and placed again under UV for 20 minutes. 156 plates were prepared, including the three replicates of each PEG concentration that were prepared for the water activity measurement. The PEG was allowed to diffuse into the agar-media for 24 hours at room temperature, after which the liquid top phase was decanted. With this method, the 0, 10, 15, and 20 %w/v PEG in the overlay solution was used to achieve 0, 5, 7.5 and 10 %w/v PEG

in the final agar media. However, from this point forward, the conditions of the plates is referred to according to the 0, 10, 15, and 20 %w/v PEG in the overlay solution.

As described in 2.3 Drought characteristics, drought can be stated as water potential, calculated from the water activity via Equation 1. The water activity of PEG infused Petri-dishes was measured with an AquaLab CX-2 water activity meter (Gemini B.V., no date).

Treated cellophane sheets were then added before the plates were inoculated. The cellophane sheets were prepared by cutting them into suitable sizes, and boiling them with 1g/L EDTA for 20 min. The sheets were then washed three times with distilled water and autoclaved twice in water. Under sterile conditions, the cellophane was placed onto the Petri dishes under a sterile bench after which the Petri dishes were placed under UV for 20 minutes. The cellophane sheets hinder the mycelium from growing into the agar and therefore allow easier post-growth handling for harvest, biomass assessment, RNA extraction and microscopic evaluation. Nutrients can be taken up through the cellophane sheet from the medium. Plates were inoculated the next day with one fungal plug per plate taken from the pre-grown fungal plates (without cellophane). Plates were incubated during the growing period in a growth chamber at 15°C constant temperature in darkness. Fungal growth was measured once a week with a ruler into two orthogonal directions across the growing fungal colony, and each growth-stage was marked with a pen, visible in the photos in Figure 8. Before analysis, outliers such as plates with irregular or absent growth were removed from the study. The replicate-average of the final growth at week four was compared between the isolates and the PEG treatment conditions.

3.2.2 Qualitative photographic analysis of drought treatment

After four weeks of growth, the mycelium was photographed with a regular camera and with a stereomicroscope. The photographs were analysed for perceived segmentation, colour, and hyphal denseness. The microscopy images were taken at 25- and 80-times magnification using a Leica stereomicroscope. Due to time-limitations, only three out of the four replicates were photographed with the microscope and analysed. A qualitative analysis was made based on branching, straightness, and hyphal denseness.

The microscope images of the *S. variegatus* isolate that showed the smallest and the largest difference in growth, respectively, between the extreme treatment 0 and 20% PEG were processed in Fiji (Schindelin *et al.*, 2012) and analysed. The image processing included changing the image type to 8-bit and adjusting the brightness and contrast with an automated setting (specific settings for each image). Each image was scaled and cropped to squares of 2.25 mm² in three places at points close to the edge without including the ends of the hyphae (Figure 2). This was done for a comparable analysis, where different amounts of empty space in the pictures due to differences in how the plate was placed during microscopy was avoided. The direction of growth was then analysed in each of the cropped images with the 'Directionality' function (Analyse → Directionality). The Local gradient orientation method was used.

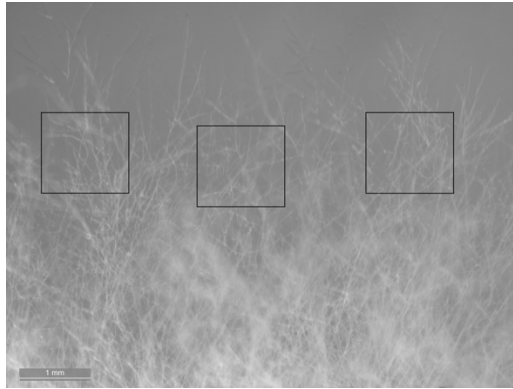


Figure 2. An example of how the images were cropped at three places in squares of 2.25 mm² close to the outer edges of the hyphae. Photo specifically shows the *S. variegatus* Kat19 0% PEG sample A.

The results from the Directionality analysis constituted directionality histograms including a gaussian fit, and a table including the direction (°), dispersion (°) and the goodness. The direction reports the centre of the gaussian, the dispersion reports the standard deviation of the gaussian fit, and the goodness reports the goodness of the gaussian fit (from 0 to 1, where 1 is good and 0 is bad). The number of peaks in the histograms were manually assessed, and the average directions were calculated from the absolute values. A Student T-test was conducted on the absolute directions to determine if there is a significant difference between the 0%- and 20% PEG treated samples in either isolate. Significance was rejected for p-values above 0.05.

3.3 Reference gene expression analysis

3.3.1 Harvest and grinding

After four weeks of growth, fungal mycelium was harvested by scraping the mycelium from the cellophane with a scalpel. The mycelium was weighed in 2 mL Eppendorf tubes. The tubes were flash frozen in liquid nitrogen and kept at -70 °C until processing.

The frozen samples were grinded with 5 mm steel beads (Qiagen). The beads had been cleaned by washing and leaving them in 10 N sodium hydroxide overnight, after which they were rinsed, autoclaved, and left to dry at 180 °C over the weekend. Before grinding, the sample holders were also placed in liquid nitrogen to keep the samples frozen throughout the grinding process. The samples were grinded in a Retsch MM 400 Mixer Mill at 3x 30 seconds and 30 Hz. Between the runs, the caps of the sample tubes were occasionally switched in the case that cracks were visible to ensure they did not break. After grinding, the samples were quickly placed back in liquid nitrogen and the steel beads were removed from all samples.

Both growth diameter and harvest weight at four weeks were analysed with two-factor analysis of variance (ANOVA) with replication in Excel (version 16.80). The null hypothesis of not significant difference was rejected if $F > F_{crit}$ and the P-value $> \alpha$ for an α of 0.05. The samples that showed a significant difference were further analysed with a post-hoc Tukey Honestly Significant Difference (HSD) test via https://astatsa.com/OneWay_Anova_with_TukeyHSD/ (Vasavada, 2016). Boxplots of the final growth and weights at harvest after four weeks of growth were made via the website <http://shiny.chemgrid.org/boxplotr/> (Development Core Team, 2013).

3.3.2 RNA extraction

For the extraction 100 mg fungal powder was weighed. For the RNA extraction, Qiagen RNeasy Mini Kits (ID: 74104) were used. For lysis, the frozen samples were mixed with 450 µl RLC buffer containing 20 µl 2M DTT. After vigorous vortexing the solution was then transferred to the Qias shredder columns and centrifuged for two minutes at 17 000 g. The supernatant was carefully moved to new tubes and mixed by pipetting with ½ volume of 95 % ethanol. The mixture was placed on the RNA binding columns and were centrifuged for 15 seconds at 8000 g. The columns were washed with 350 µl RW1 by centrifuging at 8000 g for 15 seconds.

For DNA removal, in a separate tube, 10 µl DNase I and 70 µl RDD buffer per reaction were mixed, and 80 µl of the solution were carefully pipetted to the centre of each RNA extraction column. After 15 minutes of incubation at room temperature, the columns were washed with 700 µl RW1 buffer via centrifugation at 8000 g for 15 seconds. The columns were then washed twice with 500 µl RPE buffer at 8000 g, first by centrifuging for 15 seconds, and then for two minutes. The columns were placed in new tubes and dried by one minute centrifugation. Finally, the RNA was eluted by adding 30 µl RNase-free water in the centre of each column and centrifuging for one minute at 8000 g. The eluted samples were placed on ice.

3.3.3 RNA quantification

The concentrations of the extracted RNA samples were measured with a ThermoScientific NanoDrop ND-1000 Spectrophotometer. RNase-free water was used as a blank, and a 1.5 µl drop of each sample was used for measurement. The sensor was wiped clean in-between measurements.

3.3.4 RNA quality analysis by gel-electrophoresis

The quality of the RNA from the extraction needed to be assured. For this reason, the RNA quality was analysed by visualising the results with gel-electrophoresis.

The gel mould and combs were washed with dishwashing soap and wiped clean with an RNase decontamination solution. A 1 % agarose gel in 1x TAE buffer was prepared and microwaved in 1-minute intervals until boiling. 1 µl/50 ml gel Gelgreen visualisation agent was added, and the solution was stirred before it was poured into the mould. The combs were assembled, and the gel left to solidify for 40 minutes. The gel mould and solidified gel were placed in the electrophoresis chamber with 1x TAE buffer.

The samples were prepared by adding 286-1900 ng RNA, 10 µl of diethylpyrocarbonate treated, autoclaved water (DEPC treated water), and 2 µl 6x TriTrack DNA loading dye (ThermoFisher Scientific, R1161). The samples were mixed by pipetting. The 10 µl of the samples were pipetted into the wells of the gel, and the electrophoresis was run at 130 V for 50 minutes until sufficiently separated.

The results were visualised with a Molecular Imager Gel Doc XR system high-resolution gel imaging system camera connected to Quantity One 1-D analysis software. Samples that showed clear signs of RNA degradation were excluded in the following steps.

3.3.5 Primer Design

To investigate gene expression in the mycelium by qPCR, stable reference genes are required. Selecting potential reference genes, designing efficient primers and testing reference gene stability is therefore required. The present study investigated such primers and reference genes. Sequences of known reference genes in *S. luteus* (Ruytinx, Remans and Colpaert, 2016) and *L. bicolor* (Chowdhury *et al.*, 2022) were used to search for homologs in *S. variegatus* on Mycocosm. The mRNA sequences of the homologous genes were used to design two pairs of primers for each gene in Primer3 (Rozen and Skaletsky, no date).

- Histone H4 (Mycocosm protein ID 1412056) was chosen by homology to LbHistone_H4 by best hit from tBlastN on model transcripts of *S. variegatus*
- Actin (protein ID 1530716) was chosen by homology to *S. luteus* CE100950_107466 (protein ID 100951)
- Proteasome (prot ID 1387536) was chosen by homology to *S. luteus* AM085168.
- Tubulin (protein ID 1512177) was chosen by homology to *S. luteus* AM085177 (protein ID 2000143)
- Ubiquitin (protein ID 1390168) was chosen by homology to *L. bicolor* LbUbiquitin (protein ID 446085)

For these reference genes, a total of 20 primers were designed. Two sequences for each gene, for which one forward primer and one reverse primer were designed, see Table 3.

Table 3. Primer sequences of each reference gene.

Reference gene	Sequence name	Forward primer sequence 5'-3'	Reverse primer sequence 5'-3'
Histone	His1	CCCGTGGTGTCTTAAGATCT	TGACAGTTTCCGCTTTGCA
	His2	GGTGTCAAGCGTATCTCTGG	GTTTTCCGCTTTGCATGCTC
Actin	Act1	AATGTTGTGTGTGTCGGGTGG	GTGCGACGATCTTGACCTTC
	Act2	TATCGTCATGGACTCCGGTG	ACCGCGCTCAATCAAGTTTT
Proteasome	Prot1	GCGCACCTCCTACTTGATTG	CCTCGACCTCAGCAATTTCCG
	Prot2	TGTGGTGGCAGATAATCGGT	CAATCAAGTAGGAGGTGCGC
Tubulin	Tub1	CCTCTAGGCAGTCTCTTCCG	CCCTCCGTGTAGTGTCTTT
	Tub2	GACGCTCAAACCTCTCCACAC	CACAGCAAGTTTACGCAGGT
Ubiquitin	Ubq1	CGGGTTTGAGTGGGATCCTA	TGCGGTGTTTGTATTTCCGGG
	Ubq2	GCACAGCGGCTTTTACTCAA	TAGGATCCCCTCAAACCCG

The primers were ordered from Lab Life Nordic AB.

3.3.6 cDNA synthesis

cDNA was produced from the extracted RNA with an iScript cDNA Synthesis kit (Bio-Rad, no date) from 1 µg RNA per reaction according to the manufacturer's instructions. The cDNA samples were kept at -20°C until further use.

3.3.7 Primer Specificity Test by conventional PCR and gel-electrophoresis

Primer specificity was tested by conventional PCR. An aliquot of each cDNA sample was combined into one mixture and the mixture was diluted to 1/10. The 20 primers were dissolved to 100 μ M and diluted separately to 1.6 μ M in DEPC treated water and vortexed. A mastermix was prepared containing 3.75 μ l of 2 mM dNTP, 1.5 μ l of 10x DreamTaq Green buffer (ThermoFisher Scientific), 1 μ l of the combined cDNA mixture, and 6.5 μ l of DEPC treated water per primer. 13.65 μ l of the mastermix was distributed to separate tubes. 0.625 μ l of each primer in a primer pair and 0.1 μ l DreamTaq (ThermoFisher Scientific) was added to each of the tubes. The tubes were hastily spined down in a mini centrifuge before they were placed in the Thermal Cycler with the following protocol:

1. Initial denaturation at 95°C for 3 minutes
2. Denaturation at 95°C for 30 seconds
3. Hybridization at 56°C for 30 seconds
4. Elongation at 72°C for 20 seconds
5. Final elongation at 72°C for 4 minutes
6. Hold at 4°C

Steps 2-4 were repeated 34 times.

A gel for gel-electrophoresis was prepared according to the previous protocol. 1 μ l GeneRuler DNA Ladder (ThermoFisher Scientific), 1 μ l TriTrack DNA Loading Dye (6X, ThermoFisher Scientific), and 4 μ l DEPC water were combined for the ladder. The ladder or 10 μ l of each of the PCR products were pipetted into the gel chambers. The electrophoresis was run at 130 V for 50 minutes. The gel was then visualised with the gel imaging system camera. Primers showing specificity were used in the following efficiency test.

3.3.8 Primer Efficiency Test by qPCR

The efficiencies of the primers on the cDNA stands were studied through qPCR. The combined 1/10 cDNA mixture was sequentially diluted five times with a factor five. The qPCR plate was prepared with one primer pair per row. Each row contained samples with the five dilutions in technical duplicates and a duplicated blank containing DEPC water instead of cDNA. One mastermix per primer was prepared containing SyberGreen and each primer in a primer pair. 7.5 μ l SyberGreen and 5.5 μ l of the primer pair were pipetted into the wells of each row. Thereafter, 2 μ l of the cDNA dilutions were added to all wells in each row but two, into which water was added instead. the plate was sealed with a plastic film and the PCR run on a CFX Connect Real-Time PCR Detection System with the following protocol:

Amplification:

1. 95°C for 3 minutes
2. 95°C for 10 seconds
3. 56°C for 10 seconds
4. 72°C for 20 seconds
5. Read fluorescence
6. 95°C for 10 seconds

Steps 2-5 were repeated 39 times.

Melting curve:

1. 65°C to 95°C in 0.1°C increments, reading fluorescence after each step

After assessing the standard- and melting curves, primers showing satisfying efficiency (85-100%) were used for further analysis of reference gene stability.

3.3.9 Reference gene stability analysis by quantitative PCR

Expression of each reference gene was investigated in all cDNA samples by quantitative PCR (qPCR). One mastermix per primer was prepared, containing 7.5 μ l SYBR Green mix and 2.75 μ l of each primer in a primer pair per reaction. The mastermix was distributed to the wells, after which 2 μ l of the 1/10 cDNA from the respective isolates and conditions (growth on 0 or 20% PEG) were pipette into the respective wells. For non-template controls (NTCs), 2 μ l of water was added instead of the cDNA. The plastic film was attached to seal the PCR plate and the qPCR was run with the same protocol as for the Primer Efficiency Test. A boxplot was made to visualise the gene expression with the technical means of the Cq values by using <http://shiny.chemgrid.org/boxplotr/> (Spitzer *et al.*, 2014). A single-factor ANOVA with replication was used in Excel (version) to find significant differences between the isolates and conditions within each primer. The null hypothesis of no significant difference was rejected if $F > F_{\text{crit}}$ and the P-value $> \alpha$ for an α of 0.05. The Cq Mean values were analysed in the web-based program RefFinder found at <https://blooge.cn/RefFinder/> (Xie *et al.*, 2012; Xie, Wang and Zhang, 2023). The stability was analysed with the tools normFinder and Genorm, as found in Figure 16 (Vandesompele *et al.*, 2002; Andersen, Jensen and Ørntoft, 2004).

4. Results

4.1 Phylogenetic analysis of AQPs

The AQP repertoire in the *Suillus* genus was analysed and compared to AQPs of other ECM fungi. 18 sequences were categorised as outliers due to lack of transcript sequences in MycoCosm or having four or fewer transmembrane domains. These sequences were therefore removed from dataset 1 (D1) (Table 4). After exclusions, D1 contained a total of 1352 sequences. As seen in the phylogenetic tree of D1 (found in 6.1 Appendix A – Phylogenetic tree of Dataset 1) three clusters were inferred by the reference proteins, with Cluster III containing more sequences than the other two clusters. As the reference protein of Cluster IV was not found in the dataset, no proteins were assigned to this cluster. Important to note is that two of the clades in the phylogenetic tree of D1 have separate nodes to the clades that contain the reference proteins. These clades are the bottom clade in Cluster II, and the bottom clade of Cluster I. The categorization of these clades is thus less certain, and reference proteins within these clades should be found to assign them to clusters with more certainty.

128 sequences (47 from *S. variegatus*, 49 from *S. luteus* and 32 from *S. bovinus*) from D1 were included in the curated dataset (D2). When creating the phylogenetic tree in IQTree, the program selected a best fit model based on the specific dataset which was then used for tree inference. The best fit model for D2 that was selected by IQTree was JTT+G4. The phylogeny of D2 in Figure 3 shows three clusters after pruning the tree of visible outliers. As shown in the figure, all three *Suillus* species were represented in each of the three clusters. Cluster I (Orthodox AQPs) contained 15 sequences of *S. variegatus*, 20 of *S. luteus* and 3 of *S. bovinus*. In Cluster II (Aquaglyceroporins) 7 sequences were from *S. variegatus*, 10 were from *S. luteus* and 10 from *S. bovinus*. Finally, Cluster III (Facultative AQPs) had 25 sequences were from *S. variegatus*, 19 were from *S. luteus* and 19 from *S. bovinus*. As no sequence of a reference protein for Cluster IV was found, no blast could be performed. Interestingly all sequences were represented in clusters I-III, entailing Cluster IV AQPs (fungal XIPs) were absent from the dataset.

S. variegatus
S. luteus
S. bovinus

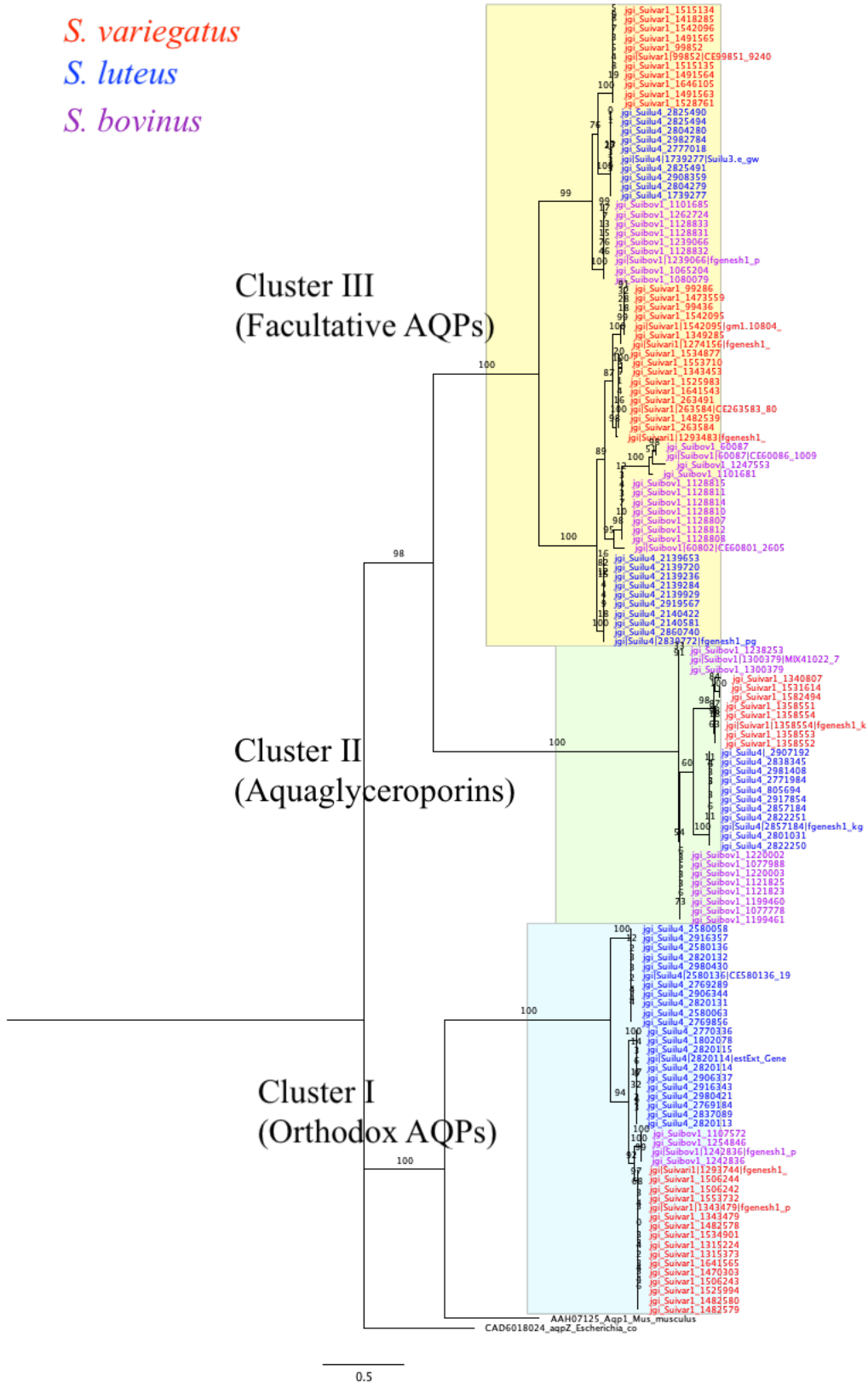


Figure 3. Phylogenetic tree of the aquaporins (AQPs) from the three *Suillus* species (*S. variegatus*, *S. luteus*, *S. bovinus*) of Dataset 2 with clustal categorisation (Cluster I: Orthodox AQPs, Cluster II: Aquaglyceroporins, Cluster III: Facultative AQPs). Made with FigTree.

Table 4 shows a list of the proteins that were excluded from D1 and D2.

Table 4. Proteins that have been excluded from the dataset 1. Dataset 1 was used to build dataset 2. Thus, exclusions were made in both datasets unless otherwise specified.

Protein ID	Reason for exclusion
Suivar1_1396569	No transmembrane region
Suivar1_341180	No Transcript, only 1 transmembrane region
Suivar1_341121	Only 2 transmembrane regions
Suibov1_60865	Only 4 transmembrane regions
Suibov1_1174494	Only 3 transmembrane regions
Suibov1_882950	No Transcript, only 3 transmembrane regions
Suivar1_265508	No Transcript
Suivari1_905565	No Transcript
Suivar1_1582490	No Transcript
Suibov1_60855	No Transcript
Suilu4_2139199	No Transcript
Suivar1_99239	No Transcript
Suivar1_99416	No Transcript
Suivar1_263452	No Transcript
Rusear1_990666	Outlier in phylogenetic tree of D1
Rusear1_967985	Outlier in phylogenetic tree of D1
Tubma1_294999	Outlier in phylogenetic tree of D1
LacbiDR170_1_1086723	Outlier in phylogenetic tree of D1

Surprisingly, many of the 128 *S. variegatus*, *S. luteus* and *S. bovinus* AQPs (D2) had identical protein- and transcript sequences. Therefore, protein- and transcript alignments were made for D2 in order to group all genes that have identical sequences (6.2 Appendix B – Sequence categorisation). The groups were made for two main reasons: (1) to analyse the topology and sequences more easily (fewer sequences needed to be individually analysed as 100% identity entails the same topology and sequence throughout each group), (2) to get a better perception on the number of different AQP proteins in each cluster and species. When these groups were made, each group containing sequences with 100% identity on protein- and transcript level, sequences that were found in Cluster I (figure 2) comprised nine groups (Figure 4), Cluster II comprised eight groups, and Cluster III comprised 22 groups. However, although proteins could be 100% identical on both protein- and transcript level, more of the proteins differed on gene-level, due to codon redundancy. Thus, when groups were made to contain the same proteins on protein-, transcript- and gene-level, Cluster I contained 18 groups, Cluster II contained 13, and Cluster III contained 42 groups. It was decided to continue the analysis based on the groups made from protein- and transcript identity. Within Cluster I, there are four groups of *S. luteus* AQPs, two groups of *S. variegatus* AQPs and three groups of *S. bovinus* AQPs. In Cluster II, there is only one group for *S. luteus*, five groups for *S. variegatus*, and two groups for *S. bovinus*. Cluster III has four groups for *S. luteus*, nine groups for *S. variegatus*, and equally many for *S. bovinus*. Some areas of the transcript sequences were conserved in all clusters, some were cluster-specific, and some were species- and cluster-specific.

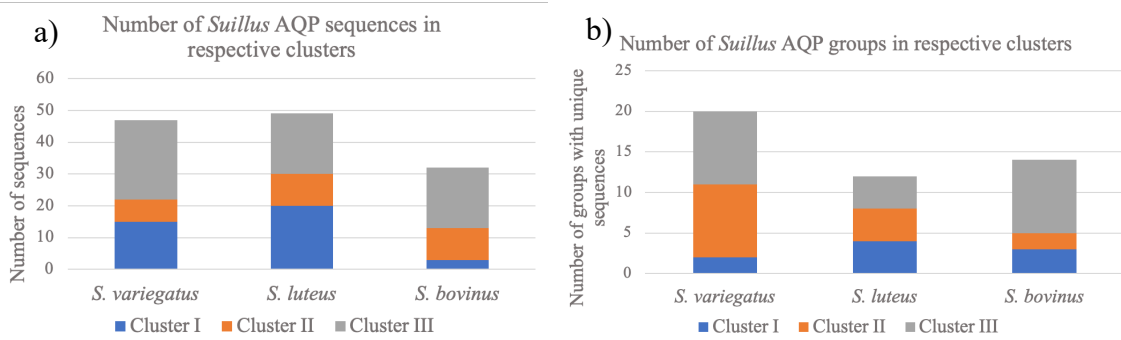


Figure 4. a) Number of aquaporin sequences of each cluster per species. b) Number of unique aquaporin sequences (groups) of each cluster per species.

4.1.1 Aquaporin topology

To check whether all identified genes would form a correct pore structure, we assessed transmembrane topology (Figure 5) as well as the presence and positions of NPA residues (Table 5). For the groups based on protein- and transcript level, the topology throughout each group was the same. All groups in Cluster I have six transmembrane domains (TMD), Cluster II has six TMDs in all groups but one, and Cluster III has six TMDs in all groups but two. All groups have both C and N termini inside the cytoplasm. The C-terminus of Cluster II is slightly longer than for Cluster I and Cluster III. The C-terminus is of similar length (ca 50 amino acids, AA) for Cluster I and III, but more variable for Cluster III than for Cluster I. The N-terminus loop of Cluster II is shorter (or no loop is present) and more variable than the C-terminus. The N-terminus of Cluster I is shorter (ca. 25 AA) and less variable than for Cluster II. In Cluster III, the N-terminus is longer (ca. 50 AA) and less variable than for Cluster II. Specifically, the sequences of *S. bovinus* in Cluster III seem the most variable.

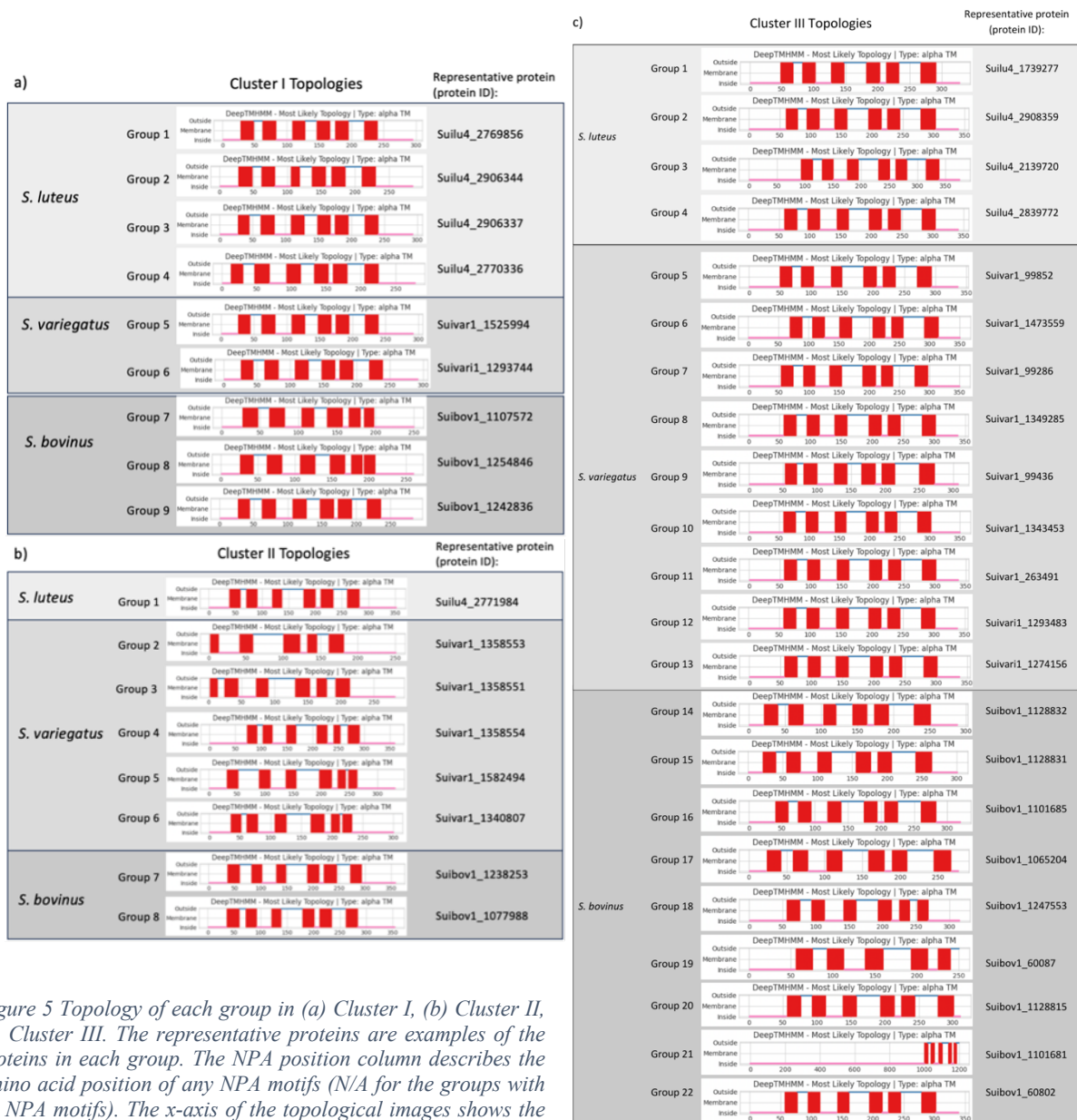


Figure 5 Topology of each group in (a) Cluster I, (b) Cluster II, (c) Cluster III. The representative proteins are examples of the proteins in each group. The NPA position column describes the amino acid position of any NPA motifs (N/A for the groups with no NPA motifs). The x-axis of the topological images shows the number of amino acids.

Examples of the 3D models made in YASARA are visualised in Figure 6. The topologies of the predicted models were found to be comparable to that of Figure 1. summarises the model template results from Swiss-Model and the motifs of the two NPA-positions in loop B and loop E according to Figure 1.

Table 5. Cluster, group, and protein ID describes the protein that was used for the model search. The model template describes the protein used in the automated comparative modeling. The GMQE is the Global model evaluation value which describes the overall model quality measurement from 0 and 1 (1 indicating the highest expected quality). Motifs in the NPA-positions shows the motifs that are present in the two (aligned) positions, in loops B and E respectively, that usually contain the NTP motif according to literature.

Cluster and group	Protein ID	Model Template	GMQE	Motifs in the NPA-positions (aligned). Loop B, Loop E
Cluster I Group 1	Suilu4_2769289	A0A1B7N9C5.1.A Organism: AM-OR11-026	0.86	89NPN, 201NTA
Cluster I Group 5	Suivar1_1641565	A0A1J8PX25.1.A Organism: Rhizopogon vesiculosus	0.88	89NPN, 201NTA
Cluster I Group 8	Suibov1_1242836	A0A0D0BEJ5_9AGAM Organism: Rhizopogon vesiculosus	0.87	89NPN, 201NTA
Cluster II Group 1	Suilu4_2822251	A0A0D0BEJ5.1.A Organism: UH-Slu-Lm8-n1	0.89	174NPA, 312NTA
Cluster II Group 3	Suivar1_1358551	A0A0D0BEJ5.1.A Organism: UH-Slu-Lm8-n1	0.87	174NPA, 312NTA
Cluster II Group 8	Suibov1_1220003	A0A0C9VWQ9.1.A Organism: UH-Slu-Lm8-n1	0.89	174NPA, 312NTA
Cluster III Group 2	Suilu4_2804280	A0A0C9VWQ9.1.A Organism: MD-312	0.87	1065NPA, 1196NPA
Cluster III Group 5	Suivar1_1528761	A0A0C9VWQ9.1.A Organism: MD-312	0.84	1065NPA, 1196NPA
Cluster III Group 7	Suivar1_99286	A0A1B7MJ40.1.A Organism: AM-OR11-026	0.85	1065NPA, 1196NPA
Cluster III Group 16	Suibov1_1262724	A0A1J8QUU6.1.A Organism: Rhizopogon vesiculosus	0.89	1065NPA, 1196NPA
Cluster III Group 20	Suibov1_1128812	A0A1B7MJ40.1.A Organism: AM-OR11-026	0.89	1065NPA, 1196NPT

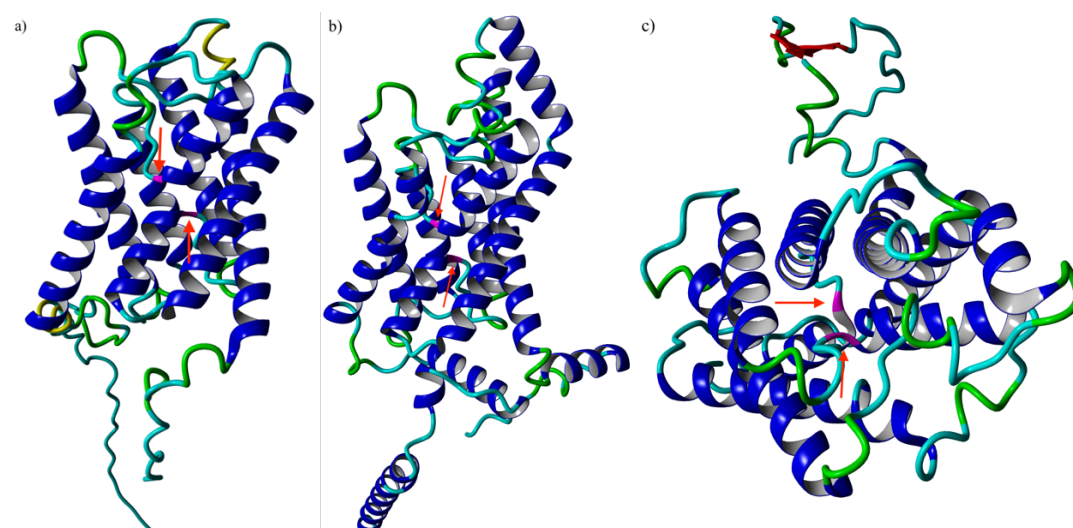


Figure 6. a) Model of *Suilu4_2769289* from Cluster I, group 1 shown with cytoplasmic side at the bottom, and extracellular at the top of the image. b) Model of *Suibov1_1220003* from Cluster II, group 8 shown with cytoplasmic side at the bottom, and extracellular at the top of the image. c) Model of *Suibov1_1128812* from Cluster III, group 20 shown from extracellular perspective. Shown in Magneta (red arrows) are the (a) 89NPN and 201NTA, (b) NPA and 236NTA, (c) NPA and 250NPT motifs.

The NPA/NPA-substitution positions (according to the aligned AA) are conserved within each cluster but differ between each cluster (Table 5). In Cluster I, the positions are occupied by an NPN substitution in loop B, and an NTA substitution in loop E across all groups, in Cluster II they are occupied by an NPA motif in loop B, and an NTA substitution in loop E across all groups. Cluster III is more diverse, with NPA motifs in both positions other than the exceptions of an NPV and an NPT substitution in loop B of group 7 and loop E of group 20, respectively. However, these are the only substitutions in Cluster III, as the remaining groups contain the aligned NPA motifs in both loops. The remaining NPA sequences found in Cluster I and Cluster III according to Figure 5 a) and c) are not found in loop B or E and do not serve the same function. Only Cluster I contains the Cluster I-specific NPN motif according to literature. None of the groups in either cluster contained the Cluster I-specific NSA motif in any of the NPA-positions and none had an NSF substitution which was found in literature. In summary (Table 6), the NPA motif is well conserved throughout all sequences, with certain substitutions that are mainly cluster-specific (rather than species specific), and the topologies of the protein sequences show consistency to what has been found in literature (Figure 1).

Table 6. Summary of the most important findings from the phylogenetic analysis of AQPs in the *Suillus* genus.

Cluster	Groups	Topology remarks	Loop B	Loop E
Cluster I	All	6 TMDs, shorter N-terminus	NPN	NTA
Cluster II	All	6 (5) TMDs, variable & shorter N-terminus, longer C-terminus	NPA	NTA
Cluster III		6 (5) TMDs, longer N-terminus, C-terminus variable	NPA	NPA
	7	6 TMDs	NPV	NPA
	20	6 TMDs	NPA	NPT

4.2 Fungal growth trial

4.2.1 Water potential

As the objective was to investigate drought sensitivity of the species *S. variegatus*, *S. luteus* and *S. bovininus*, simulated drought conditions needed to be ensured. Therefore, the water potential of the plates with different concentrations of PEG (0, 10, 15, 20% in overlay solutions) were assessed.

The water activities of the agar plates were measured in replicates of three for each of the four PEG treatment conditions. The water activity was converted to Ψ_w via equation 1. The standard deviation was calculated, and a T-test was conducted against the 0% condition for each of the PEG concentrations, see Table 7. The table shows that there were only statistically significant differences in Ψ_w between 0% and 20% PEG.

Table 7. Water activity and water potential analysis of PEG treatment conditions.

%w/v PEG	Water activity (Aw)		Temp (°C)	Ψ_w (Mpa)	Average (Mpa)	Std Dev	Student T-test
0	0.997	0.998	23.8	-4.07	-2.26	1.57	
0	0.999		24.4	-1.36			
0	0.999		23.9	-1.35			
10	0.996	0.997	24.3	-5.43	-4.52	1.57	0.15
10	0.996		23.8	-5.43			
10	0.998		23.4	-2.71			
15	0.994	0.996	24.1	-8.15	-5.88	2.08	0.07
15	0.996		23.7	-5.42			
15	0.997		23.9	-4.07			
20	0.996	0.995	23.8	-5.43	-7.26	1.59	0.02
20	0.994		25	-8.18			
20	0.994		24.7	-8.17			

4.2.2 Measured growth

To compare drought sensitivity of different isolates of *S. variegatus*, *S. luteus* and *S. bovinus* osmotic stress was simulated and fungal growth (diameter and weight) was compared after four weeks. No data is shown for *S. bovinus* since 50% of the plates had either not grown at all or had become contaminated. Lack of growth was also found in three of the 0% PEG *S. luteus* KS1 isolate samples. Overall, significant effects (ANOVA p-value <0.05) on diameter growth (Table 8) and weight (Table 9) were only observed for one isolate of *S. variegatus*, namely LV1, but not for the other isolates or for *S. luteus* (Figure 7). Growth of LV1 was reduced by 28% in the 20% compared to the 0, 10 and 15 % PEG condition. Weight, however, was significantly reduced by 23% only between 0 and 20% PEG of LV1 (Figure 7).

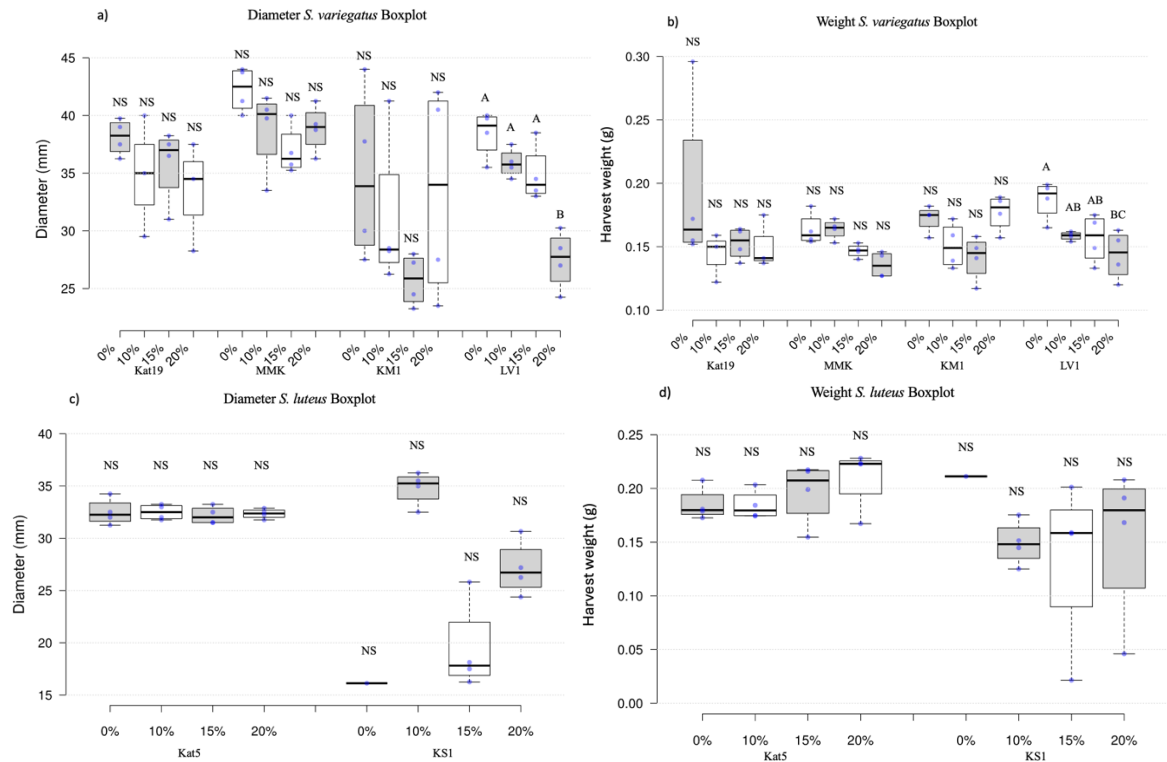


Figure 7. Boxplot of (a), (c) the growth diameter and (b), (d) the weights at harvest of the (a) (b) *S. variegatus* isolates and (b) (c) *S. luteus* isolates after four weeks of growth. NS is written for the isolates within which no significant difference in growth/diameter was found by the Tukey Honestly Significant Difference test. Unique letters above the bars of the LV1 isolate in a) and b) refer to significant difference (Two-factor ANOVA and Tukey HSD with $p < 0.05$).

Table 8. Post-hoc Tukey Honestly Significant Difference results for the growth diameters of *S. variegatus* isolate LV1.

Treatment pairs (% PEG)	Tukey HSD Q statistic	Tukey HSD p-value	Tukey HSD inference
0% vs 10%	2.38	0.37	Insignificant
0% vs 15%	3.31	0.14	Insignificant
0% vs 20%	10.16	0.0010	** $p < 0.01$
10% vs 15%	0.93	0.90	Insignificant
10% vs 20%	7.79	0.0010	** $p < 0.01$
15% vs 20%	6.86	0.0020	** $p < 0.01$

Table 9. Post-hoc Tukey Honestly Significant Difference results for the harvest weights of *S. variegatus* isolate LV1.

Treatment pairs (% PEG)	Tukey HSD Q statistic	Tukey HSD p-value	Tukey HSD inference
0% vs 10%	3.62	0.10	Insignificant
0% vs 15%	3.88	0.07	Insignificant
0% vs 20%	5.53	0.01	** $p < 0.01$
10% vs 15%	0.25	0.90	Insignificant
10% vs 20%	1.91	0.55	Insignificant
15% vs 20%	1.65	0.65	Insignificant

4.2.3 Qualitative photographic analysis of drought treatment

To assess potentially distinct growth patterns of the fungal species at the different drought conditions, a quantitatively analysis was conducted on photographs of the fungal plates after four weeks of growth. There was a similar pattern of segmentation of growth on all plates (Figure 8), where the pigmentation of the mycelium is more intense in the centre of the mycelial

mat than on the outer edges. The segmentation of the pigmentation aligns with the markings for each of the growth measurements. Another common trend between the isolates is that the colour seems to differ between the treatments. The colour is more visible from the backside of the plates and intensifies with increased PEG concentration (Figure 8). A third observation regards the thickness of growth of the outermost layer of hyphae. Common across all isolates is that this layer seems to be thicker for the 20% PEG concentrations and sparser in the 0% PEG samples.

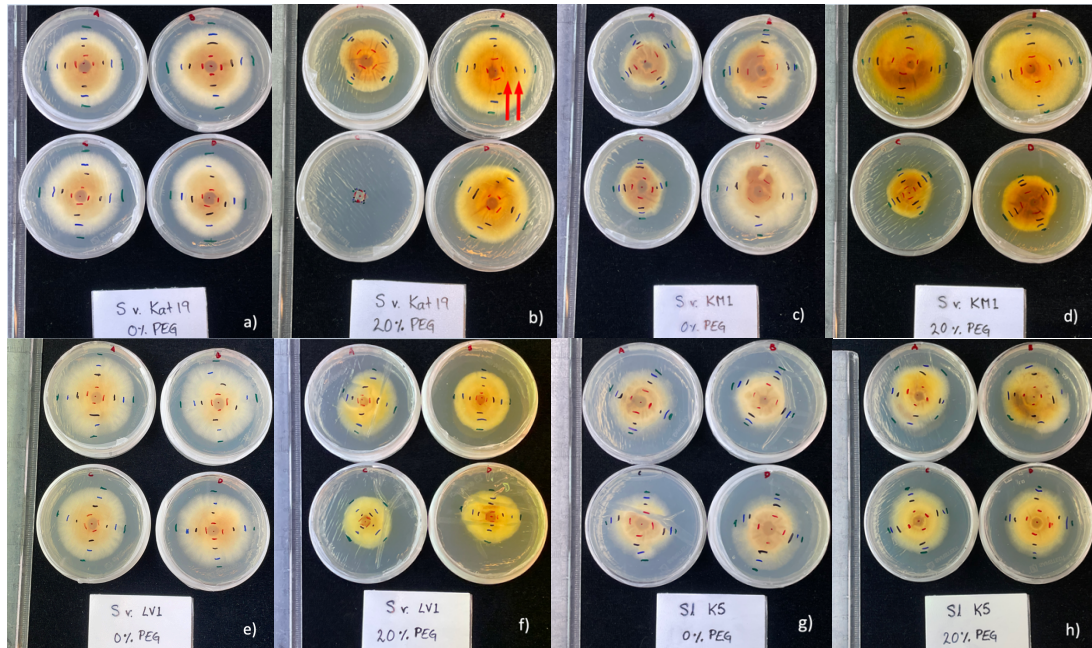


Figure 8. 0% and 20% PEG samples of the isolates (a, b) *S. variegatus* Kat19, (c, d) *S. variegatus* KMI, (e, f) *S. variegatus* LV1 and (g, h) K5. Photos taken from the bottom of the petri-dishes after four weeks of growth. Growth segmentation is indicated by red arrows in image b), although it is visible in all pictures.

As mentioned in 3.3 **Error! Reference source not found.**, the effect of the PEG concentration was exhibitive in the increasingly shrivelled inoculation plugs with increasing PEG concentration. For example, on 20% PEG the plug was noticeably smaller and darker (more shrivelled) than at 0% PEG (figure 7). This phenomenon was even more clear in the plugs of the first batch of mycelium, which was prepared on larger plates (9cm VS 6cm diameter in the second batch). Figure 9 shows the plates of two isolates where the plug (dark circle in the centre of the mycelium) is clearly more shrivelled (darker and smaller) in the 20% PEG plate than the 0% PEG plate.

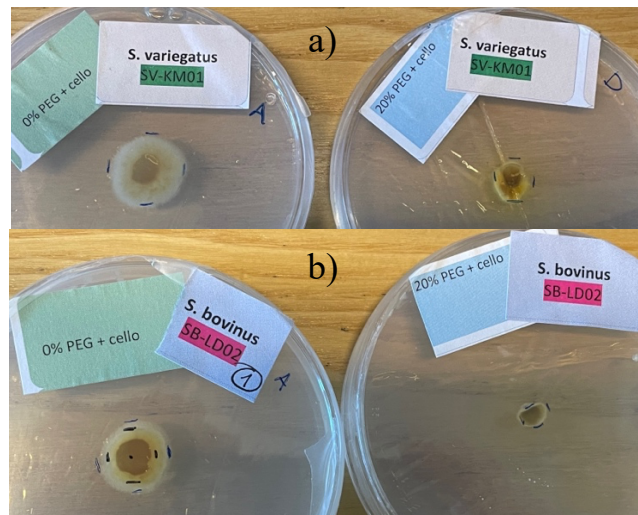


Figure 9. Plates of a) *S. variegatus* KMI and b) *S. bovinus* LD2 from first batch of cultivation. Mycelium at one week of growth. Left in image is the 0% PEG plates, and on the right is the 20% PEG plates.

To further assess possible differences in hyphal growth between the treatments, the stereomicroscope images of the cultures at four weeks of growth were analysed. No apparent differences were found between the treatment conditions regarding branching, straightness, and thickness of growth from observing the photos qualitatively (Figure 10).

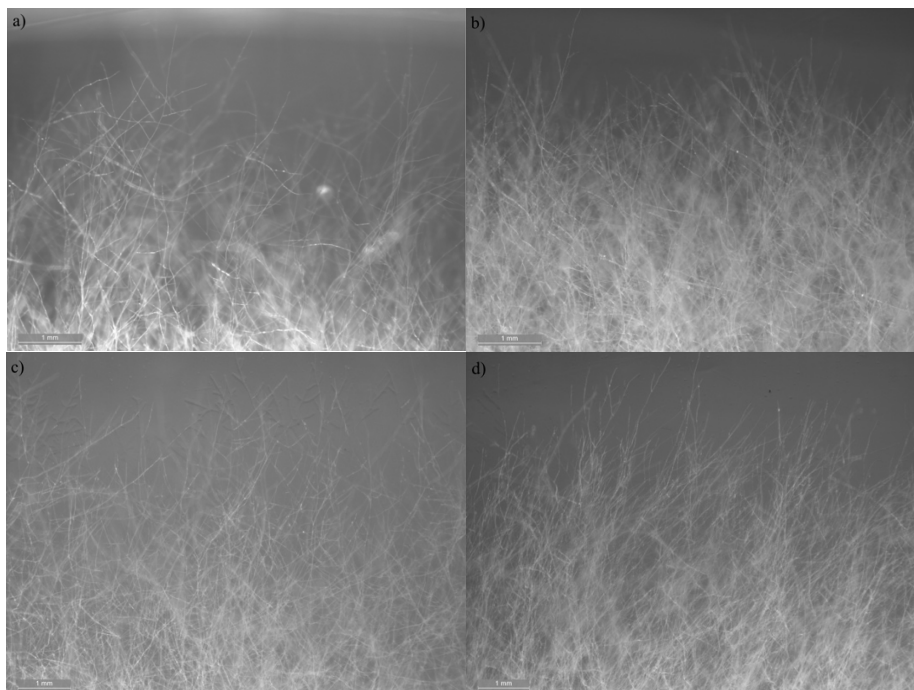


Figure 10. Stereomicroscopic images at 80-times magnification. (a, c) 0% PEG condition and (b, d) 20% PEG conditions of the isolates (a, b) *S. variegatus* Kat19 and (c, d) *S. variegatus* LV1. Grayscale 8-bit images with scalebar.

As the only isolate whose growth was significantly impacted by PEG was *S. variegatus* LV1, hyphal directionality close to the edge of the colony was compared between 0 and 20% for this isolate and for another one that was not influenced by the treatment, namely *S. variegatus* K19 (Table 10). Only 15 of the 36 measurements received goodness values above 0.5. Both isolates had a higher average absolute direction of the samples treated at 20% PEG than those treated at 0% PEG: 75 VS 66° for *S. variegatus* LV1 and 90 VS 71° for *S. variegatus* K19. However, this was only significant for K19 (Student T-Test p-value = 0.02). The T-test was, nevertheless, based on the directions which in turn were based on the gaussian fit, and the majority of the

gaussians fit values received a goodness of fit of less than 0.5. The number of peaks were very similar among all samples.

Table 10. Results from the Directionality test in Fiji on the 80-times magnified stereomicroscopic images of the *S. variegatus* LV1 and K19 samples treated at 0%- and 20% PEG. The Goodness reports the goodness of the gaussian fit of the histograms. Goodness above 0.5 are marked in green, and below 0.5 are marked in orange.

Sample	Goodness	Av. Dis (°) ¹	#Peaks	StdDev ²	Av. Dir (°) ³	Av. Dir (°)
LV1 20% PEG C3	0.19		1			
LV1 20% PEG C2	0.55	11	1	5	87	
LV1 20% PEG C1	0.26		1			
LV1 20% PEG B3	0.31		1			
LV1 20% PEG B2	0.48	18	1	2	67	75
LV1 20% PEG B1	0.49		1			
LV1 20% PEG A3	0.71		1			
LV1 20% PEG A2	0.83	17	1	3	70	
LV1 20% PEG A1	0.82		1			
LV1 0% PEG C3	0.6		2			
LV1 0% PEG C1	0.57	28	2	8	67	
LV1 0% PEG B3	0.64		1			
LV1 0% PEG B2	0.42		2	5	70	66
LV1 0% PEG B1	0.61	21	1			
LV1 0% PEG A3	0.49		1			
LV1 0% PEG A2	0.32		2	15	62	
LV1 0% PEG A1	0.33	17	1			
Kat19 20% PEG D3	0.23		1			
Kat19 20% PEG D2	0.47		2	20	87	
Kat19 20% PEG D1	0.57	24	1			
Kat19 20% PEG B3	0.42		1			
Kat19 20% PEG B2	0.48		1	24	97	90
Kat19 20% PEG B1	0.35	24	1			
Kat19 20% PEG A3	0.25		1			
Kat19 20% PEG A2	0.48		1	7	84	
Kat19 20% PEG A1	0.52	16	1			
Kat19 0% PEG C3	0.73		1			
Kat19 0% PEG C2	0.8		1	14	59	
Kat19 0% PEG C1	0.39	24	1			
Kat19 0% PEG B3	0.78		1			
Kat19 0% PEG B2	0.29		2	3	71	71
Kat19 0% PEG B1	0.75	14	1			
Kat19 0% PEG A3	0.45		1			
Kat19 0% PEG A2	0.48		1	4	83	
Kat19 0% PEG A1	0.48	13	1			

¹ Av. Dis, Average Dispersion

² StdDev, Standard Deviation

³ Av. Dir, Average Absolute Direction

Overall, significant effects of growth on diameter and weight were only *S. variegatus* LV1. However, possible drought effects on pigmentation and thickness of growth of the outermost

layer of hyphae are common across all samples. More subtle effects such as branching, straightness, and thickness of the hyphae were difficult to assess qualitatively, but nevertheless, they were not observed. A more quantitative analysis would be important to verify these findings. Differences between treatments in hyphal directionality close to the edge of the colony was significant for K19 rather than LV1. As K19 had not been found to have significant differences in diameter and weight between treatment conditions, this may point to that there can be more subtle reactions to drought. However, the goodness of the data this result was based on was too low to conclude anything definite.

4.3 Reference gene expression analysis

4.3.1 RNA quality analysis by gel-electrophoresis

The study intended to analyse AQP gene expression in the different growth condition. This was, however, not possible due of the high number of AQP detected in *Suillus* and their sequence similarity that requires other approaches ahead of qPCR analysis not possible within the time frame of this thesis. In the future, if or when this approach is performed, it will however require stable reference genes. Therefore, it was decided to design and validate reference genes for *S. variegatus*. RNA was extracted from mycelium on 0 and 20% PEG from four *S. variegatus* isolates. Figure 11 RNA in the samples MMK 0% D, MMK 20% A, C, D, and LV1 0% C had been degraded (Figure 11). Moreover, sample K19 20 % A was of very low concentration. The MMK isolate as well as the LV1 0% C and K19 20 % A samples were therefore excluded from further experiments. The remaining samples had two clear bands each, indicating successful RNA extraction without breakdown products.

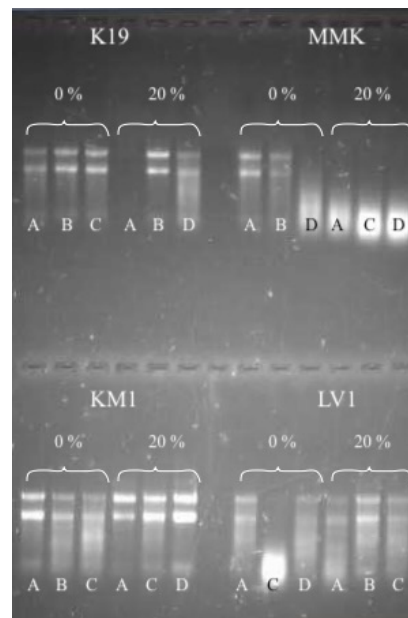


Figure 11. Results of RNA quality analysis by gel-electrophoresis.

4.3.2 Primer Specificity

To assess primer specificity and since for each of the five reference genes two primer pairs had been designed, PCR was first conducted with all primer pairs on a mixture of cDNA from the successfully extracted RNAs at two hybridization temperatures, 60°C and 56°C. Only Actin1

showed amplification at 60°C whereas at 56°C Histon1, Actin1, Tubulin1, Tubulin2, Ubiquitin1, and Proteasome1, showed amplified fragments, albeit to differing degrees. Thus, the efficiency analysis was conducted on these six primerpairs.

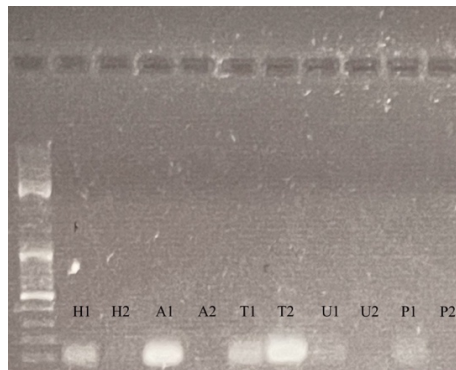
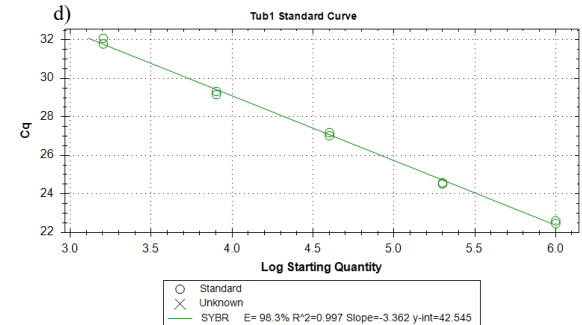
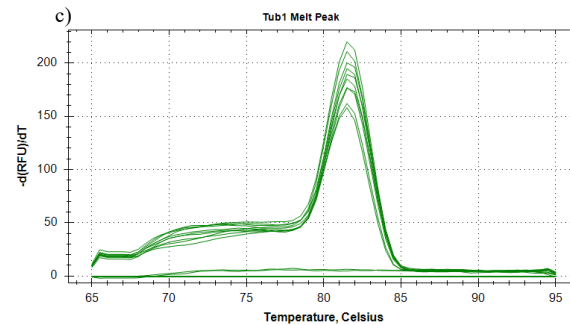
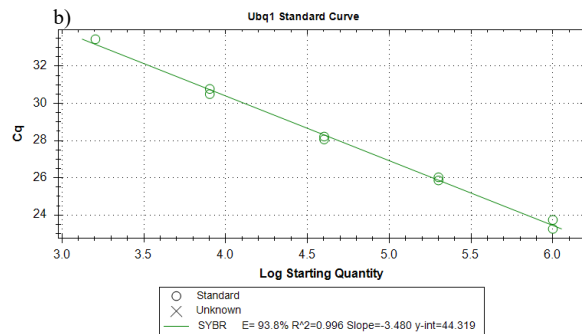
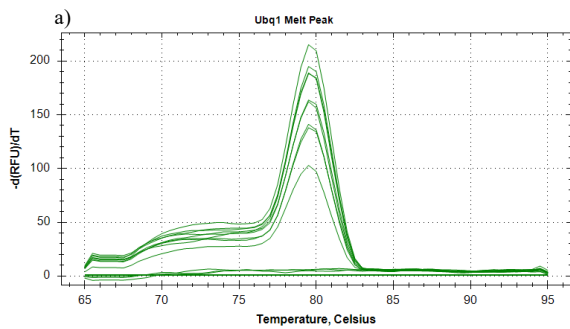


Figure 12. Results of primer specificity analysis by gel-electrophoresis. (H1/2 – Histone primer pair 1 and 2, A1/2 Actin primer pair 1 and 2, T1/2 - Tubulin primer pair 1 and 2, U1/2 - Ubiquitin primer pair 1 and 2, P1/2 - Proteasome primer pair 1 and 2)

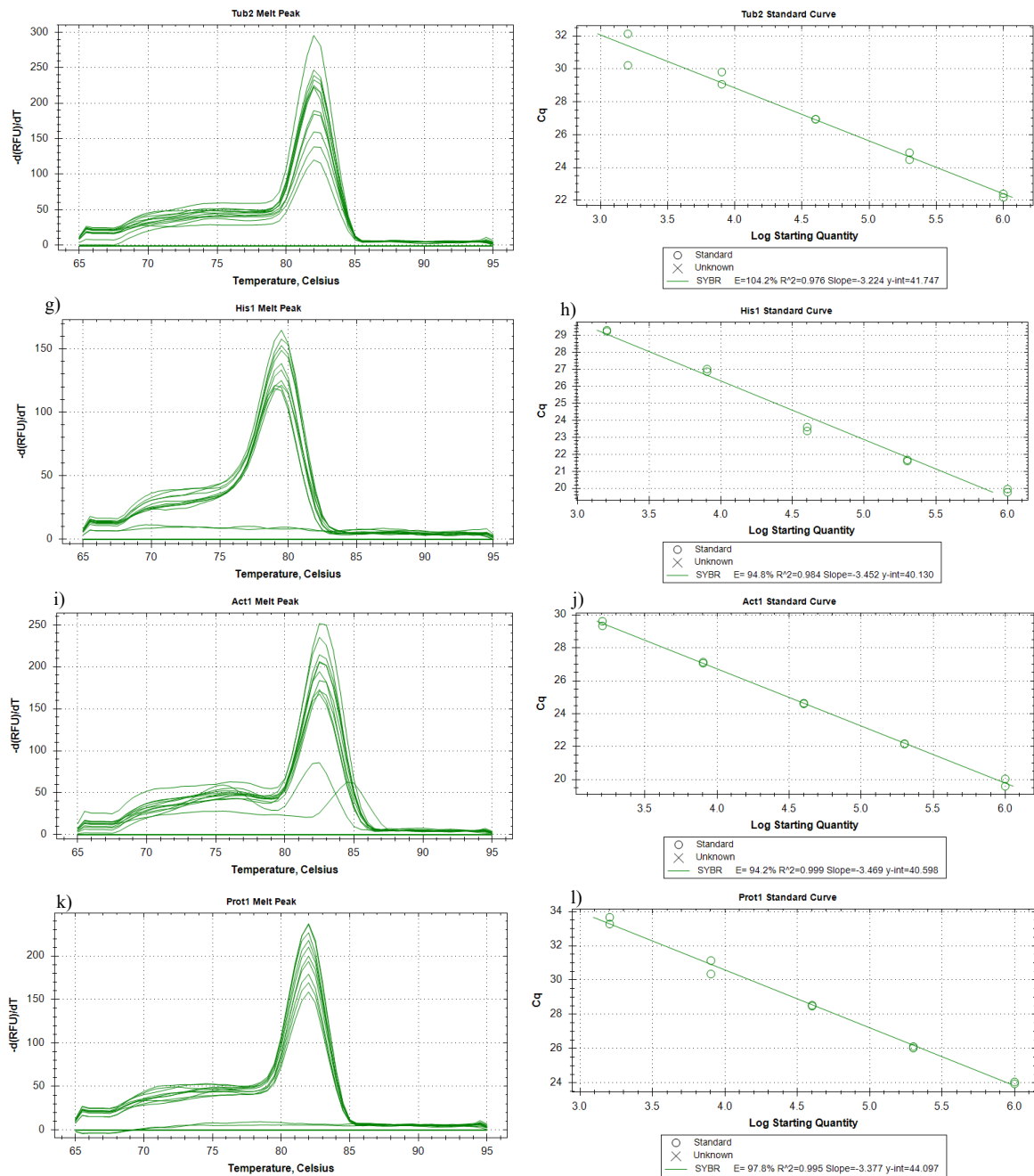
4.3.3 Primer Efficiency

The primer efficiency was tested on the cDNA samples with qPCR. Figures 13-19 show the melting peaks and standard curves from the qPCR of each primer. The Melt Peak figures show single clearly defined peaks without shoulders and artifacts, and absence of amplification in Non-Template Controls (NTCs), with exception of Actin1. The Standard Curves show the efficiency of the primers as well as the R² values of the slopes. The R² coefficient of correlation is >99% for all primers except for Tubulin2 and Histon1 which have an R² of 97.6% and 98.4% respectively.



e)

f)



Figures 13. (a, c, e, g, i, k) Melt Peaks and (b, d, f, h, j, l) Standard Curves for of the primers (a, b) Ubiq1, (c, d) Tub1, (e, f) Tub2, (g, h) His1, (i, j) Act1 and (k, l) Prot1.

The efficiency of the primers visible in Figures 13 are also summarised in Table 11. There is a high efficiency for all primers, with highest values for Tubulin2, Tubulin1 and Proteasom1. The lowest values are found for Ubiquitin1, Actin1 and Histon1, yet still sufficient.

Table 11. Primer efficiency summarised from the qPCR results.

Primer	Efficiency (%)
Ubiquitin1	93.8
Tubulin1	98.3
Tubulin2	96.8
Histone1	94.8
Actin1	94.2
Proteasom1	97.8

4.3.4 Reference gene expression and stability

qPCR was used to investigate the expression of each reference gene in all tested cDNA samples. Due to contamination, lack of growth of certain samples, and time limitations, only the *S. variegatus* isolates were used for analysis of reference gene stability. The Quantification Cycle (Cq) standard deviation between technical replicates was found to be less than 1 cycle for all samples, with three exceptions which were excluded from the study. Looking at gene expression in general (Figure 14), the highest expression levels (lowest Cq values) were found for Actin1 and Histone1, and the lowest for Ubiquitin1 and Proteasom1. However, all genes were highly expressed throughout all sample conditions.

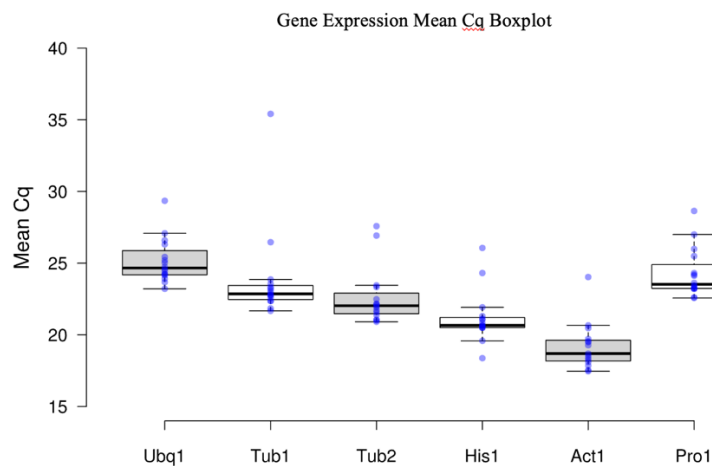


Figure 14. Boxplot visualising the gene expression by the Cq means of the technical replicate. Made in <http://shiny.chemgrid.org/boxplot/>.

A column graph of the Cq means is shown in Figure 15. Throughout the primers, the KM1 20% PEG sample shows higher values, indicating that there was probably less RNA in the cDNA synthesis. No statistically significant differences between the isolates and conditions within each primer were found by the ANOVA.

Cq Mean - Reference gene expression

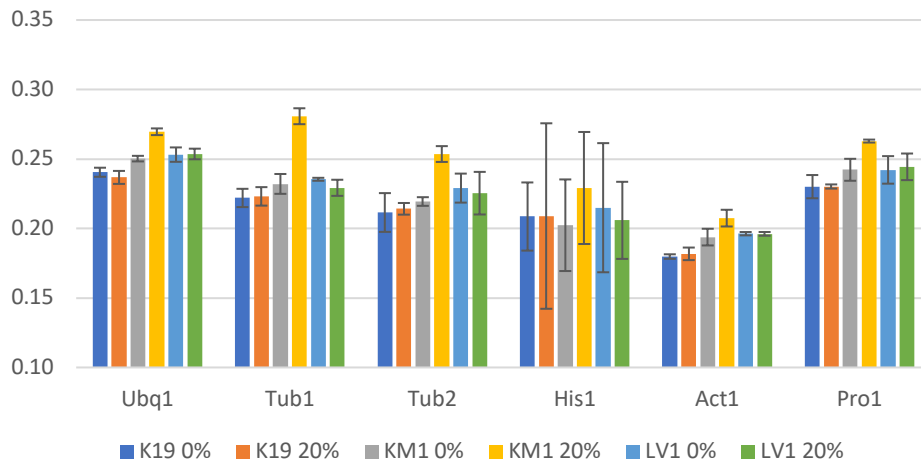


Figure 15. Column graph showing the Cq Mean values of each isolate and condition within the six primers as well as the standard deviations of the biological replicates.

The results of the primer stability analysis are visible in Figure 16. Ubiquitin1 and Tubulin1 were found to have the highest stability, and Proteasom1 found to have the lowest.

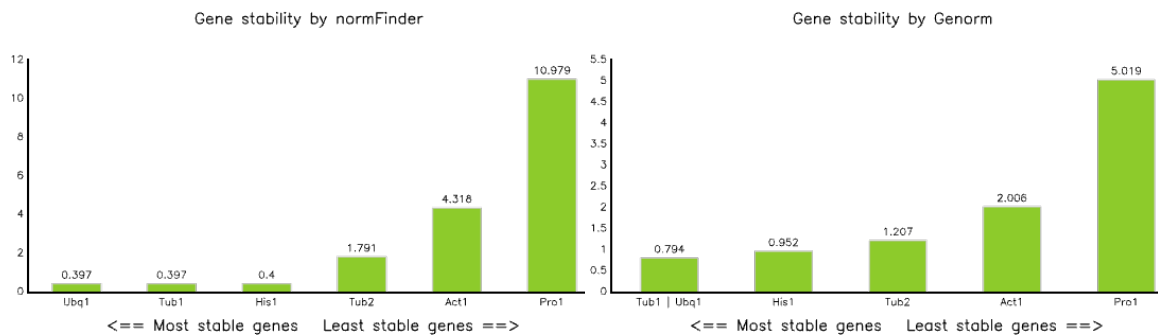


Figure 16. Gene stability results produced with the two methods normFinder (left) and Genorm (right) in the web-based PCR analysis program RefFinder (Vandesompele et al., 2002; Andersen, Jensen and Ørntoft, 2004).

Taken together, efficient primers were successfully designed for stable reference genes that can be used for future qPCR-based gene expression studies in *S. variegatus*.

5. Discussion

5.1 AQP repertoire in the *Suillus* genus

A main objective of the study has been to explore the attributes of the aquaporin gene collection in the *Suillus* genus, focusing on understanding the type and degree of their variation both within this genus and in other groups. As many of the AQPs had identical protein- and transcript sequences groups were made (8.2 Appendix B – Sequence categorization) where each group contained sequences of 100% identity. This was done based on the assumption that it is a sequencing artifact that so many identical sequences were found. However, this assumption may be false and should be investigated further. An alternative explanation could be that it is due to a biological phenomenon. To address this question, it would be recommended to clone all AQP sequences, to amplify the DNA in bacteria after which each gene could be sequenced and identified. Next, Thermal Asymmetric InterLaced-PCR (TAIL-PCR) could be conducted as this method helps identify unknown sequences flanking a known part of the DNA. This would give information on how many genes are present in the genome, thus, if the multiple identical AQP sequences are in fact due to the presence of numeral sequences in the same genome.

Cluster I (orthodox AQPs), Cluster II (Fps-like aquaglyceroporins and others), and Cluster III AQPs (facultative fungal AQPs/Yfl054-like AQPs) were represented in all three species of *Suillus*. No sequence of a reference protein for Cluster IV was found a blast search could not be performed. However, all the sequences were identified as members of Cluster I, II or III. Thus, it was concluded that none of the *Suillus* sequences were Cluster IV proteins. This may either entail that there are no Cluster IV AQPs in *Suillus* or that no Cluster IV AQPs have been sequenced in the genus. No literature was however found on the subject. These findings align with the hypotheses made that Cluster I-III AQPs would be found to a higher extent than Cluster IV AQPs. This hypothesis was made simply due to the fact that Cluster IV are more rare according to literature (Nehls and Dietz, 2014). However, the hypothesis that Cluster I AQPs would be found to a larger extent in *S. variegatus* due to the presumed drought resilience of the species, and the cluster's potential for water uptake was refuted. Contradictory results were found (Figure 4). *S. luteus* was found to have slightly more AQP sequences than *S. variegatus*, however, *S. variegatus* was found to have the largest number of unique sequences out of the three species. This could be due to drought adaptivity, but, as only a small segment of these are Cluster I AQPs, the case for a higher drought adaptivity is not strong. In fact, *S. variegatus* have the fewest unique Cluster I AQPs out of the three species. To be able to draw conclusions related to drought sensitivity, further research is needed regarding the correlation between the AQP cluster, the NPA substitutions and the drought resilience of the mycelium. Possibly, the rationale that *S. variegatus* would be more drought resistant, which lie behind the hypothesis, is incorrect. Furthermore, it may be that the Cluster I AQPs are more expressed in

conditions of drought although the genetic coding for the proteins are fewer. This would need to be investigated with analysis of gene expression of AQPs in the different conditions. Furthermore, the proportion of Cluster III (also called facultative fungal AQPs or Yfl054-like AQPs) in D2 was comparable to D1, as it was the largest cluster in both cases.

Substitutions of the NPA motif was expected, as they have been found in literature, and especially in fungi (Nehls and Dietz, 2014). The specific substitutions found in the present study align with what has been reported in literature, with one exception in Cluster III. The present study found that Cluster I contained the NPN and NTA motifs in loop B and E and that Cluster II contained the motifs NPA and NTA in loop B and E respectively in all groups. These respective substitutions are all reported in literature (Xu, Cooke and Zwiazek, 2013a). Interestingly, Xu et al. state that the substitutions found in Cluster II often relate to a lower water permeability and that Cluster I is predicted to have a higher water permeability (Xu, Cooke and Zwiazek, 2013a). The present study has found the very same substitution in loop E of both Cluster I and Cluster II, but the differences in the substitutions of loop B between the two clusters may result in a slightly different selectivity of the protein, which should be investigated further. Finally, the Cluster III protein motifs were found to differ among the groups and even within species. NPA was found in both positions for most groups, with the exceptions NPV in loop B of one group of *S. variegatus*, and NPT in loop E of one group of *S. bovinus*. This was similar to the findings of Xu *et al.*, who found NPA motifs in both positions in Cluster III proteins of *L. bicolor*, with an occasional NPV substitution in loop B. However, they did not report an NPT substitution in loop E which was found herein. Exploring the patterns of loops B and E across all *Suillus* species and analysing them against typical growth conditions and drought resilience of the species might yield intriguing insights regarding how the different substituted NPA motifs may affect water permeability and drought resistance of the mycelium.

The topology of the proteins was similar across all clusters, with a few distinctions. Literature states that the proteins of all clusters generally consist of six TMDs (Xu, Cooke and Zwiazek, 2013a), which was also found in the present study. Exceptions included a few cases of five TMDs in Clusters II and III, which has also been reported in literature. Also, the length of the termini was generally consistent with the report by Xu et al., with the main exception that the present study found that the N-terminus of Cluster II AQPs was mostly relatively shorter, whilst Xu et al. found this to be relatively longer (Table 12).

Table 12. Remarks of the termini of each cluster found in the present study compared to what is reported by Xu et al. (Xu, Cooke and Zwiazek, 2013a).

Cluster	Termini remarks, present study	Termini remarks, Xu et al.
Cluster I	Shorter N-terminus, medium-long C-terminus	Shorter N-terminus, long C-terminus
Cluster II	Variable & shorter N-terminus, longer C-terminus	N- and C-termini relatively long
Cluster III	Longer N-terminus, C-terminus variable but medium length	Long N-terminus, C-terminus medium-long

To encapsulate, the motifs and topological results from the present study are generally consistent with literature, with a few interesting divergences regarding the NPA motif. Delving into the significance of the different motifs found in loops B and E and the qualities they relate to could be a compelling area of study.

5.2 Technical improvements for growth study

The primary aim of this study was to explore the impact of simulated drought conditions on the growth behavior of the fungal species. In extension, this entailed constructing a reproducible, quantifiable, and realistic method for simulating drought conditions. The degree of success of this ambition merits further discussions.

Throughout the two batches of cultured fungi, there were quite a few samples that did not grow at all. In fact, 17 of the samples of the second batch did not grow and were therefore excluded. This may be due to the inoculation plug not containing an equal quality of mycelium. When stamping out the inoculation plugs from the precultured plates, the outermost layer of the hyphae was taken, if possible. However, at times, there was not enough mycelium to do so. Especially for the second batch, as the inoculation plugs were taken from the same precultured plates for both batches. In contrast, there was only one sample that did not grow in the first batch. Thus, the quality of the plug may have varied across the samples, especially in the second batch.

Osmolovskaya et al. reports that a Ψ_w of <-0.8 MPa is generally recognised as an indication of drought stress, with values of $\Psi_w < -1.2$ MPa can be considered medium to medium-high drought stress (Osmolovskaya *et al.*, 2018). Based on this, the water activity results showed indications of medium high levels of drought stress even at 0% PEG, as the measured Ψ_w ranged between -2.26 MPa for 0% PEG to -7.26 MPa for 20% PEG. Osmolovskaya et al. continues to write that that an overlay solution model with PEG8000 can achieve down to -0.47 MPa to -3.02 MPa, which is well surpassed by the results herein. It is, however, worth to note that the relative difference in Ψ_w may be reasonable although the absolute values seem extreme. Using PEG as drought simulation

Keeping in mind that the concentration of PEG in the agar is half of the concentration in the overlay solution, the water activity was measured to 0.998 for 0% PEG, 0.997 for 5% PEG, 0.996 for 7.5% PEG and 0.995 for 10% PEG. These results are lower than those reported by Ninni et al. as they had found a water activity of 0.999 for 5% PEG, and 0.998 for 5% PEG. They achieved a water activity of 0.994 at 20% PEG (Ninni, Camargo and Meirelles, 1999). The difference between these measurements may reflect on the experimental apparatus used in the study, due to its advanced age and prolonged period without maintenance as this could potentially influence the accuracy and precision of the measurements.

Due to the surprisingly low water potentials achieved by the present method, it would be beneficial to compare the results herein to those of similar studies. However, very rarely has the method using a PEG overlay solution on agar media been used to simulate drought, and even more rarely have both the PEG concentrations and the subsequent water potentials been documented. No studies could be found where the present method was used on mycelial fungi. A study by van der Weele et al. used essentially the same method as the present study by growing *Arabidopsis thaliana* in PEG-8000 infused 1.2% agar. They reported that the agar of their 'well-watered' control without PEG had a water potential of -0.10 MPa, and that their PEG-treated plates reached water potentials of between -0.5 to -1.2 MPa. No PEG concentrations were specified in the overlay solution. Weele et al. reported significant differences in the growth of the stress-induced and control-plants (van der Weele *et al.*, 2000). Furthermore, the two studies by Liu et al. and Navarro-Ródenas et al., respectively, have grown different fungi on filters on liquid medium treated with a range of concentrations of PEG-6000. The studies both found significant differences in growth of the fungi between the treatment

groups and both studies both found that a range of 0-20% of PEG-6000 concentrations corresponded to -0.16 to -1.07 (Navarro-Ródenas *et al.*, 2011; Liu *et al.*, 2021). The literary comparisons are not ideal, but they do seem to show that the concentrations of PEG-8000 that were added in the present study should not correspond to the water potentials that were measured. The seemingly high measurements lead to further suspicion of the apparatus used in the study.

As there were clear visual effects of a difference in Ψ_w between the inoculation plugs of the 0% PEG and 20% PEG conditions in the first batch, as seen in Figure 9, the second batch only included concentrations up to 20% PEG. However, shrinkage-effects on the plug that had been noticed in batch 1 were not as evident in the second batch, although still present. The reason for the shrinkage effect to be less evident in the second batch is unknown. However, as the plates were smaller in the second batch, the inoculation plug was larger relative to the amount of agar medium. As the plug itself contained water, one can speculate that the reason that the shrinkage was less evident in the second batch was due to the larger ratio of plug per medium in the smaller plates. Future studies should include measurements of the plug itself to quantitatively assess the shrinkage of the inoculation plug.

Although a difference in water potential between the treatment conditions can be deduced from the relative difference in Ψ_w and the shrinkage effect on the plug, a lower Ψ_w might have been beneficial to obtain statistically significant differences in the growth and weight of the mycelium between the treatment groups. Ninni *et al.* described that due to the ratio between the terminal OH groups and the molecule, PEG of a lower molecular weight depress water activity more than those of a high MW (Ninni, Camargo and Meirelles, 1999). As it might not be possible to experimentally achieve a desired concentration of PEG with PEG 8000 due to its high density, it may be advised to investigate lower Ψ_w with PEG 6000.

5.3 How does drought stress influence *Suillus* mycelium growth?

The research question *How does simulated drought stress affect the growth patterns of the fungal species?* has been explored by subjecting *S. variegatus*, *S. luteus*, and *S. bovinus* to three degrees of drought and measuring possible effects in a number of ways. No conclusions could be drawn from any of the isolates of the *S. bovinus* species or the *S. luteus* KS1 isolate, as this only had one replicate at 0% PEG. Additional studies are required to draw conclusions on the drought resilience of these isolates. Thus, comparisons of the effects of drought on the three species could not be explored, thus leaving part of the research question unanswered. Particular drought resilience in regard to growth of the mycelium was not found in any isolates, with one exception being LV1 of *S. variegatus* (*however, there were more isolates of this species included in the study*). Interestingly, the diameter measurements showed differences between each of the lower-drought conditions and the 20% PEG condition, but for the weight measurements, there was only a significant difference between the 0% and 20% PEG conditions. This seems to entail that the mycelium grew thinner overall, either sparser or with thinner hyphae, for each of the higher concentrations of PEG. This could be a due to an adaptation linked to dehydration, to achieve an increased area of exploration for water foraging.

The observation of increased hyphal density at the edge of the colonies on high PEG concentration (Figure 8) raised the question whether drought influences mycelium density in general. Studies on the effects of drought on the hyphal denseness could not be found for ECM fungi, although it has been studied in arbuscular fungi. Nevertheless, as arbuscular fungi are obligate symbionts, all such studies look at the hyphal denseness of arbuscular mycorrhizal fungi (AMF). Khalvati et al. have investigated barley inoculated with the AMF *Glomus intraradices* in well-watered and drought conditions. They found significantly higher hyphal densities in the hyphal- and root compartments under drought conditions than under well-watered conditions (Khalvati *et al.*, 2005). A study on Chinese fir by Dong et al. found that drought led to a decreased surface area available for AMF infection on the roots and that this in turn caused an increase in the mycorrhizal hyphal density. The study investigated the mycorrhiza in the top 10 cm of soil around the Chinese fir (Dong *et al.*, 2023). Although the articles may reinforce the present findings, the differences in the patterns of growth between AMF and ECM must be considered. Furthermore, contradicting results have also been found by Maitra et al. who reported that drought significantly decreased the extraradical hyphal density of AM fungi (Maitra *et al.*, 2019). It may be hypothesised that a denser hyphal net can increase the desiccation-tolerance of the mycelium, which would be especially beneficial in drought conditions. A single hypha should dry out faster than tightly packed hyphae. Such is the function of the mycobiont of lichens, which helps prolong periods of hydration of the lichen (Spribille *et al.*, 2022).

The density of the hyphae overall as well as specifically in the outermost layer, and the thickness of the hyphae are interesting factors to study closer in future drought-experiments. Image analysis to further explore these factors could not be employed in the current study, as no methods could be found that differentiated between density of hyphal growth and thickness of hypha. Furthermore, it would be interesting to analyse the length and branching of the hyphae under the different conditions. This calls for alternative methods to be selected for future endeavours. It would be interesting to use image analysis in Fiji to explore the density of the hyphae. For this, the Ridge detection plugin can be used, as this does not take the thickness of the hypha into consideration. Then, the pixels can be counted to give information regarding the density of the hyphae. However, as hyphal thickness cannot be measured from the stereomicroscope images and hyphal branching can be confounded by the overlapping hyphae in the stereomicroscope images, another method must be employed. To measure hyphal branching, length, thickness, and density more exactly, mycelium would need to be fixated (e.g. in paraformaldehyde), sectioned, stained with e.g. Wheat Germ Agglutinin, coupled to a fluorophore and then analysed with confocal microscopy. This would provide higher magnification and resolution to assess those parameters.

Interestingly, only the Kat19 isolate, which had no statistically significant difference in growth (harvest/weight), showed a significant difference in directionality between the treatment conditions 0- and 20% PEG. However, the directionality itself was based on a gaussian fit with a low goodness of fit. This brings the reliability of the directionality into question. A more robust and reliable method to assess the directionality could be to use the staining method with confocal microscopy described above, as this would yield a higher resolution. Additionally, it would be interesting to explore the difference in the results if the plug-in 'Ridge detection' were to be used before the directionality was assessed, in the case that this would achieve a greater goodness of fit.

Furthermore, the alignment of the segmentation of pigment and markings from the growth measurements shown in Figure 8 suggests that there was a fungal response to the light exposure in combination with each measurement. This may very well be true as light sensing in mycelium is tightly linked to signaling cascades and developmental pathways (Yu and Fischer, 2019). Another observation regards the increased pigmentation of the 20% PEG samples in Figure 8 compared to the 0% PEG samples. Fungal pigmentation such as melanin and carotenoids have been widely reported to function as external stress-mediators. Melanin and carotenoids contain free radical centres that allows them to act as C, by which they protect from oxidative stress related to i.e. drought as well as visible-light exposure (Lin and Xu, 2022; Li *et al.*, 2023; Naz *et al.*, 2023). Thus, the increase of pigment due to the light exposure during measurements, as well as the increase of pigmentation in the more drought-exposed samples both correlate with literature regarding the stress-mediating function of fungal pigmentation. It would be interesting to explore the types of pigmentation specifically expressed due to light- and/or drought exposure in the *Suillus* genre.

5.4 Identification of reference genes of *Suillus variegatus*

The research question *How does drought influence the gene expression profile of aquaporins, and what implications does this have for understanding the adaptive strategies for drought tolerance?* could not be explored due to large number of AQPs identified in *Suillus* and their sequence similarity, which necessitate alternative methods beyond qPCR analysis, not feasible within the timeframe of this thesis. However, the study instead explored the development of stable reference genes for qPCR analysis in *S. variegatus* to aid in future research of the initial research question. Looking at gene expression (Cq) and reference gene stability, it became clear that the most highly expressed genes are not necessarily the genes that are the most stable, as visualised by the hierarchical position of Tubulin2 in Figure 16 and Figure 14. Interestingly, Histone has the largest Cq variability across all tested cDNAs, even within the biological replicates, as seen by the error bars in Figure 14, but it is still one of the most stable genes. Another puzzling result is that although Protease seems to be equally expressed as Ubiquitin or Tubulin, it is the least stable gene by far.

The primers demonstrated specificity, evidenced by the amplification of a single product, and exhibited high efficiency, with rates exceeding 90%. Therefore, the strategy of designing primers based on both the genes of organisms that are more closely related to *S. variegatus*, such as *S. luteus*, as well as genes of organisms that are less closely related, like *L. bicolor*, is deemed successful. Although the project aim included analysis of gene expression of AQPs in the different conditions, this was not done due to the insight of the size of such a task after the identification of the number of AQP sequences in the bioinformatics part. The number of different AQPs were many more than anticipated, and their transcript sequences could have high levels of similarity over long stretches, which made the design of specific primers of such target genes impossible, as seen when putative primers were blasted against the other AQP sequences. Furthermore, given that many identical transcript sequences were identified we would first need to understand how many unique AQPs there actually are. In a future study, it would be advised to conduct RNA sequencing on samples that have been exposed to different degrees of drought. After analysing which genes are differentially regulated at the varying conditions and having confirmed AQP sequences through a cloning approach, qPCR may be used. It is also worth considering TaqMan qPCR where, in addition of a forward and reverse primer, a probe is designed that can span longer stretches of sequences (up to 30bp) and help quantify transcripts of gene families with sequences showing a higher degree of similarity. For

this reason, the design of successful primers for the reference genes will hopefully be a prosperous feat, as they can be used in this purpose. In future studies, the reference genes need also be designed for *S. bovinus* (for *S. luteus* they are available from the literature).

5.5 Conclusions

To establish a more resilient forestry, drought resistance of trees through ECM symbiotic relationships is a promising approach. This degree project has aimed to further build a foundational understanding of the drought resistance in the ECM *Suillus* genus by investigating the research questions:

- What are the characteristics of the gene repertoire of aquaporins within the *Suillus* genus, and what is the nature and extent of their divergence within and beyond the genus?
- How does simulated drought stress affect the growth patterns of the fungal species?
- How does drought influence the gene expression profile of aquaporins, and what implications does this have for understanding the adaptive strategies for drought tolerance?

The existing literature was examined to assess the current state of understanding regarding the significance of aquaporins. The gene repertoire of AQP in the *Suillus* genus was investigated and key motifs in the AQP transcript were compared within the genus and to literature. Although the expression of AQP could not be examined in different conditions of drought, insights were reached on how to explore the topic in future research.

Although only a single isolate showed significant difference in diameter and weight between the treatment conditions, there were other common trends across all isolates in more subtle reactions to the drought treatment, such as effects in pigmentation and denseness of hypha. This may suggest that drought conditions were achieved, but no differences in diameter or weight were found due to drought resilience of the isolates. However, alternative methods (or devices) should be used to measure the water activity so that this can be more robustly confirmed.

Although not a focus of the study originally, a valuable result from the present study is the development of the experimental procedure of exposing the mycelium to artificial drought. No literature was found on previous studies using the present method on mycelium, although the method itself has been regarded as optimal for drought simulation in other organisms. The method was modified to produce sterile conditions and to successfully achieve sufficient levels of drought.

Finally, the thesis study successfully designed stable reference genes for qPCR analysis in *S. variegatus* to aid in future research of the gene expressions of AQP in different conditions of drought.

In essence, this master's thesis has provided foundational understanding on the subject of drought resistance in a few species within the ECM *Suillus*. This will facilitate in future research regarding how ECM species differ in drought sensitivity, which in turn might aid in developing a resilient forestry by the recognition of which fungal species are more suitable for increasing the drought resilience of tree seedlings.

6. Future Outlook

As described, although the practice of inoculating tree seedlings with ECM fungi is old, the understanding of how ECM support outplanted tree seedlings in drought conditions and which ECM species are most suited to do so, is limited. To understand this, it is helpful to first gain insight on the drought sensitivity of the fungi themselves. Familiarity of how ECM species differ in drought sensitivity might aid in research regarding which fungal species are more suitable for increasing the trees' drought resilience.

Gaining a more comprehensive understanding of the varying degrees and mechanisms of drought resilience among ECM species can pave the way for insightful studies into the impact of ECM symbiosis on tree drought resistance. Such studies will be significant for developing effective strategies to mitigate the effects of drought on forest ecosystems. Three main research questions have, for this purpose, been suggested for future studies:

- Do fungal NPA substitutions influence their drought tolerance?
- Do the natural habitats of the fungal isolates influence their drought tolerance?
- Does AQP repertoire, expression and fungal drought sensitivity influence mycorrhizal tree performance?

Understanding the differences in aquaporin selectivity based on the substitutions of the NPA motif and the effect of these substitutions on drought sensitivity, could aid in selecting appropriate species to test for increasing the drought resilience of tree seedlings.

Exploring the natural habitats of the different ECM species may give insights into their respective preferences regarding climate and soil conditions. Understanding this, can provide conclusions of their stress resilience and adaptability capabilities, as well as inform the practicality of incorporating ECM into forestry practices to improve seedling drought resistance. Moreover, the environmental and ecological parameters that required for growth and proliferation of these ECM fungi need also to be clearly defined for the method to be effective in forestry applications.

Ultimately, while compelling advancements have been made in understanding ECM and their role in forest ecosystems, future research must delve deeper into these symbiotic relationships, especially in the context of climate change. This will not only contribute to our scientific knowledge but also aid in developing practical solutions for sustainable forestry and environmental conservation.

References

- Abbas, S. . *et al.* (2014) ‘Detection of drought tolerant sugarcane genotypes (*Saccharum officinarum*) using lipid peroxidation, antioxidant activity, glycine-betaine and proline contents’, *Journal of soil science and plant nutrition*, (ahead), pp. 0–0. doi: 10.4067/S0718-95162014005000019.
- Adams, Moss and McClure (2016) *Food Microbiology*. 4th edn.
- Agerer, R. (2001) ‘Exploration types of ectomycorrhizae: A proposal to classify ectomycorrhizal mycelial systems according to their patterns of differentiation and putative ecological importance’, *Mycorrhiza*, 11(2), pp. 107–114. doi: 10.1007/s005720100108.
- Aju, P. C., Iwuchukwu, J. J. I. and Ibe, C. C. (2015) ‘Our Forests, Our Environment, Our Sustainable Livelihoods’, *European Journal of Academic Essays*, 2(4), pp. 6–19. Available at: https://www.researchgate.net/profile/Paulinus-Aju/publication/353014874_Our_Forests_Our_Environment_Our_Sustainable_Livelihoods/links/60e4288ca6fdccb7450b8bf3/Our-Forests-Our-Environment-Our-Sustainable-Livelihoods.pdf.
- Andersen, C. L., Jensen, J. L. and Ørntoft, T. F. (2004) ‘Normalization of Real-Time Quantitative Reverse Transcription-PCR Data: A Model-Based Variance Estimation Approach to Identify Genes Suited for Normalization, Applied to Bladder and Colon Cancer Data Sets’, *Cancer Research*, 64(15), pp. 5245–5250. doi: 10.1158/0008-5472.CAN-04-0496.
- Aroca, R. and Ruiz-Lozano, J. M. (2017) *Plant Aquaporins and Mycorrhizae: Their Regulation and Involvement in Plant Physiology and Performance*. Edited by F. Chaumont and S. Tyerman. Springer International Publishing AG 2017. doi: 10.1007/978-3-319-49395-4.
- Bacelar, E. L. V. A. *et al.* (2012) *Water use strategies of plants under drought conditions, in Plant responses to drought stress, Spain, Berlin*.
- Bailey, S. N., Elliott, G. P. and Schliep, E. M. (2021) ‘Seasonal temperature–moisture interactions limit seedling establishment at upper treeline in the Southern Rockies’, *Ecosphere*, 12(6). doi: 10.1002/ecs2.3568.
- Balestrini, R. and Kottke, I. (2016) ‘Structure and development of ectomycorrhizal roots’, *Molecular Mycorrhizal Symbiosis*, pp. 47–61. doi: 10.1002/9781118951446.ch4.
- Bertoni, M. *et al.* (2017) ‘Modeling protein quaternary structure of homo- and hetero-oligomers beyond binary interactions by homology’, *Scientific Reports*, 7(1), p. 10480. doi: 10.1038/s41598-017-09654-8.
- Bienert, S. *et al.* (2017) ‘The SWISS-MODEL Repository—new features and functionality’, *Nucleic Acids Research*, 45(D1), pp. D313–D319. doi: 10.1093/nar/gkw1132.
- Bio-Rad (no date) *iScript™ cDNA Synthesis Kit*. Available at: <https://www.bio-rad.com/en-se/product/iscript-cdna-synthesis-kit?ID=M87EWZESH> (Accessed: 13 January 2024).
- Bista, D. *et al.* (2018) ‘Effects of Drought on Nutrient Uptake and the Levels of Nutrient-Uptake Proteins in Roots of Drought-Sensitive and -Tolerant Grasses’, *Plants*, 7(2), p. 28. doi: 10.3390/plants7020028.
- Bonfante, P. and Anca, I. A. (2009) ‘Plants, mycorrhizal fungi, and bacteria: A network of

interactions', *Annual Review of Microbiology*, 63, pp. 363–383. doi: 10.1146/annurev.micro.091208.073504.

Cairney, J. W. G. and Chambers, S. M. (1999) *Ectomycorrhizal Fungi Key Genera in Profile*. Edited by J. W. G. Cairney and S. M. Chambers. Berlin, Heidelberg: Springer Berlin Heidelberg. doi: 10.1007/978-3-662-06827-4.

Castaño, C. *et al.* (2023) 'Ectomycorrhizal fungi with hydrophobic mycelia and rhizomorphs dominate in young pine trees surviving experimental drought stress', *Soil Biology and Biochemistry*, 178(June 2022). doi: 10.1016/j.soilbio.2022.108932.

Chaumont, F. *et al.* (2001) 'Aquaporins Constitute a Large and Highly Divergent Protein Family in Maize', *Plant Physiology*, 125(3), pp. 1206–1215. doi: 10.1104/pp.125.3.1206.

Chowdhury, J. *et al.* (2022) 'Laccaria bicolor pectin methylesterases are involved in ectomycorrhiza development with Populus tremula × Populus tremuloides', *New Phytologist*, 236(2), pp. 639–655. doi: 10.1111/nph.18358.

Cordell, C. E. and Omdal, D. W. (1990) 'Identification, management, and application of ectomycorrhizal fungi in forest tree nurseries', *Diseases and Insects in Forest Nurseries*, pp. 143–155. Available at: https://www.researchgate.net/profile/R-Kasten-Dumroese/publication/272827883_Fusarium_disease_of_conifer_seedlings/links/54f4d42e0cf2ba6150642226/Fusarium-disease-of-conifer-seedlings.pdf#page=151.

Correia, M. *et al.* (2021) 'Land-use history alters the diversity, community composition and interaction networks of ectomycorrhizal fungi in beech forests', *Journal of Ecology*, 109(8), pp. 2856–2870. doi: 10.1111/1365-2745.13674.

Cram, M. M., Frank, M. S. and Mallams, K. M. (2012) 'Forest Nursery Pests', *United States Department of Agriculture*, pp. 20–22. Available at: https://www.researchgate.net/profile/R-Kasten-Dumroese/publication/265713887_Forest_Nursery_Pests_review/links/54ee2b060cf2e55866f22b1b/Forest-Nursery-Pests-review.pdf#page=28.

Dahlberg, A. (1997) 'Population ecology of Suillus variegatus in old Swedish Scots pine forests', *Mycological Research*, 101(1), pp. 47–54. doi: 10.1017/S0953756296002110.

Danielson, J. Å. and Johanson, U. (2008) 'Unexpected complexity of the Aquaporin gene family in the moss Physcomitrella patens', *BMC Plant Biology*, 8(1), p. 45. doi: 10.1186/1471-2229-8-45.

Development Core Team (2013) 'R: A Language and Environment for Statistical Computing. R Foundation for Statistical Computing'.

Dietz, S. *et al.* (2011) 'The aquaporin gene family of the ectomycorrhizal fungus Laccaria bicolor: Lessons for symbiotic functions', *New Phytologist*, 190(4), pp. 927–940. doi: 10.1111/j.1469-8137.2011.03651.x.

Dong, J. *et al.* (2023) 'Drought Changes the Trade-Off Strategy of Root and Arbuscular Mycorrhizal Fungi Growth in a Subtropical Chinese Fir Plantation', *Forests*, 14(1), p. 114. doi: 10.3390/f14010114.

Froger, A. *et al.* (1998) 'Prediction of functional residues in water channels and related proteins', *Protein Science*, 7(6), pp. 1458–1468. doi: 10.1002/pro.5560070623.

Gemini B.V. (no date) *AquaLab CX-2*. Available at: <https://www.geminibv.com/labware/aqualab-cx-2/> (Accessed: 13 January 2024).

Gena, P. *et al.* (2011) 'Aquaporin Membrane Channels: Biophysics, Classification, Functions, and Possible Biotechnological Applications', *Food Biophysics*, 6(2), pp. 241–249. doi: 10.1007/s11483-010-9193-9.

Gonzalez, S. *et al.* (2022) 'Mimicking genuine drought responses using a high throughput plate assay', *bioRxiv*. Available at: <https://www.biorxiv.org/content/10.1101/2022.11.25.517922v1%0Ahttps://www.biorxiv.org/content/10.1101/2022.11.25.517922v1.abstract>.

- Grigoriev, I. V. *et al.* (2014) ‘MycoCosm portal: gearing up for 1000 fungal genomes’, *Nucleic Acids Research*, 42(D1), pp. D699–D704. doi: 10.1093/nar/gkt1183.
- Groppa, M. D., Benavides, M. P. and Zawoznik, M. S. (2012) ‘Root hydraulic conductance, aquaporins and plant growth promoting microorganisms: A revision’, *Applied Soil Ecology*. Elsevier B.V., 61, pp. 247–254. doi: 10.1016/j.apsoil.2011.11.013.
- Guerreiro, S. B. *et al.* (2018) ‘Future heat-waves, droughts and floods in 571 European cities’, *Environmental Research Letters*, 13(3), p. 034009. doi: 10.1088/1748-9326/aaaad3.
- Guevara-Gonzalez, R. and Torres-Pacheco, I. (eds) (2014) *Biosystems Engineering: Biofactories for Food Production in the Century XXI*. Cham: Springer International Publishing. doi: 10.1007/978-3-319-03880-3.
- Guex, N., Peitsch, M. C. and Schwede, T. (2009) ‘Automated comparative protein structure modeling with SWISS-MODEL and Swiss-PdbViewer: A historical perspective’, *ELECTROPHORESIS*, 30(S1). doi: 10.1002/elps.200900140.
- Gupta, A. and Sankararamakrishnan, R. (2009) ‘Genome-wide analysis of major intrinsic proteins in the tree plant *Populus trichocarpa*: Characterization of XIP subfamily of aquaporins from evolutionary perspective’, *BMC Plant Biology*, 9(1), p. 134. doi: 10.1186/1471-2229-9-134.
- Hallgren, J. *et al.* (2022) *DeepTMHMM predicts alpha and beta transmembrane proteins using deep neural networks*, *Technical University of Denmark*. doi: doi.org/10.1101/2022.04.08.487609.
- Imtiaz, A. A. *et al.* (2020) ‘Screening of Mungbean Genotypes under Polyethylene Glycol (PEG) Induced Drought Stress Condition’, *Annual Research & Review in Biology*, pp. 1–12. doi: 10.9734/arrb/2020/v35i230184.
- Ishikawa, F. *et al.* (2005) ‘Novel type aquaporin SIPs are mainly localized to the ER membrane and show cell-specific expression in *Arabidopsis thaliana*’, *FEBS Letters*, 579(25), pp. 5814–5820. doi: 10.1016/j.febslet.2005.09.076.
- Islam, M. R. *et al.* (2017) ‘Morphology and mechanics of fungal mycelium’, *Scientific Reports*. Springer US, 7(1), pp. 1–12. doi: 10.1038/s41598-017-13295-2.
- Jiang, Y. (2009) ‘Expression and functional characterization of NPA motif-null aquaporin-1 mutations’, *IUBMB Life*, 61(6), pp. 651–657. doi: 10.1002/iub.203.
- Johanson, U. *et al.* (2001) ‘The Complete Set of Genes Encoding Major Intrinsic Proteins in *Arabidopsis* Provides a Framework for a New Nomenclature for Major Intrinsic Proteins in Plants’, *Plant Physiology*, 126(4), pp. 1358–1369. doi: 10.1104/pp.126.4.1358.
- Juenger, T. E. and Verslues, P. E. (2023) ‘Time for a drought experiment: Do you know your plants’ water status?’, *Plant Cell*, 35(1), pp. 10–23. doi: 10.1093/plcell/koac324.
- Katoh, K. (2023) ‘MAFFT’. Available at: <https://mafft.cbrc.jp/alignment/software/>.
- Khalid, H., Kumari, M. and Nasim, M. (2021) ‘Drought tolerance studies in in vitro grown *Camelina sativa* (L.)Crantz by exogenous application of polyethylene glycol.’, *International Journal of Advanced Research in Biological Sciences*, 8(5), pp. 80–90. doi: 10.22192/ijarbs.
- Khalvati, M. A. *et al.* (2005) ‘Quantification of Water Uptake by Arbuscular Mycorrhizal Hyphae and its Significance for Leaf Growth, Water Relations, and Gas Exchange of Barley Subjected to Drought Stress’, *Plant Biology*, 7(6), pp. 706–712. doi: 10.1055/s-2005-872893.
- Kohler, A. *et al.* (2015) ‘Convergent losses of decay mechanisms and rapid turnover of symbiosis genes in mycorrhizal mutualists’, *Nature Genetics*, 47(4), pp. 410–415. doi: 10.1038/ng.3223.
- Korkama, T., Pakkanen, A. and Pennanen, T. (2006) ‘Ectomycorrhizal community structure varies among Norway spruce (*Picea abies*) clones’, *New Phytologist*, 171(4), pp. 815–824. doi: 10.1111/j.1469-8137.2006.01786.x.
- Kretzer, A. M. and Bruns, T. D. (1999) ‘Use of *atp6* in Fungal Phylogenetics: An Example from the Boletales’, *Molecular Phylogenetics and Evolution*, 13(3), pp. 483–492. doi:

10.1006/mpev.1999.0680.

Krieger, E. and Vriend, G. (2014) 'YASARA View—molecular graphics for all devices—from smartphones to workstations', *Bioinformatics*. Netherlands, Austria: Bioinformatics 30, 2981–2982, 30(20), pp. 2981–2982. doi: 10.1093/bioinformatics/btu426.

Kruse, E., Uehlein, N. and Kaldenhoff, R. (2006) 'The aquaporins', *Genome Biology*, 7(2). doi: 10.1186/gb-2006-7-2-206.

Lalor, A. R. *et al.* (2023) 'Mortality thresholds of juvenile trees to drought and heatwaves: implications for forest regeneration across a landscape gradient', *Frontiers in Forests and Global Change*, 6. doi: 10.3389/ffgc.2023.1198156.

Larsson, A. (2014) 'AliView: a fast and lightweight alignment viewer and editor for large datasets', *Bioinformatics*, 30(22), pp. 3276–3278. doi: 10.1093/bioinformatics/btu531.

Lehto, T. and Zwiasek, J. J. (2011) 'Ectomycorrhizas and water relations of trees: a review', *Mycorrhiza*, 21(2), pp. 71–90. doi: 10.1007/s00572-010-0348-9.

Li, J. *et al.* (2023) 'Simultaneous Production of Cellulase and β -Carotene in the Filamentous Fungus *Trichoderma reesei*', *Journal of Agricultural and Food Chemistry*, 71(16), pp. 6358–6365. doi: 10.1021/acs.jafc.3c00690.

Li, S. *et al.* (2021) 'Genome-Wide Identification and Function of Aquaporin Genes During Dormancy and Sprouting Periods of Kernel-Using Apricot (*Prunus armeniaca* L.)', *Frontiers in Plant Science*, 12. doi: 10.3389/fpls.2021.690040.

Li, T. *et al.* (2013) 'First cloning and characterization of two functional aquaporin genes from an arbuscular mycorrhizal fungus *Glomus intraradices*', *New Phytologist*, 197(2), pp. 617–630. doi: 10.1111/nph.12011.

Lin, L. and Xu, J. (2022) 'Production of Fungal Pigments: Molecular Processes and Their Applications', *Journal of Fungi*, 9(1), p. 44. doi: 10.3390/jof9010044.

Liu, B. *et al.* (2021) 'Stress tolerance of *Xerocomus badius* and its promotion effect on seed germination and seedling growth of annual ryegrass under salt and drought stresses', *AMB Express*, 11(1), p. 15. doi: 10.1186/s13568-020-01172-7.

Lofgren, L. A. *et al.* (2021) 'Comparative genomics reveals dynamic genome evolution in host specialist ectomycorrhizal fungi', *New Phytologist*, 230(2), pp. 774–792. doi: 10.1111/nph.17160.

Luoranen, J., Riikonen, J. and Saksa, T. (2023) 'Damage caused by an exceptionally warm and dry early summer on newly planted Norway spruce container seedlings in Nordic boreal forests', *Forest Ecology and Management*, 528, p. 120649. doi: 10.1016/j.foreco.2022.120649.

Mahpara, S. *et al.* (2022) 'The impact of PEG-induced drought stress on seed germination and seedling growth of different bread wheat (*Triticum aestivum* L.) genotypes', *PLOS ONE*. Edited by S. Farooq, 17(2), p. e0262937. doi: 10.1371/journal.pone.0262937.

Maitra, P. *et al.* (2019) 'Effect of drought and season on arbuscular mycorrhizal fungi in a subtropical secondary forest', *Fungal Ecology*, 41, pp. 107–115. doi: 10.1016/j.funeco.2019.04.005.

Marjanović, Ž. *et al.* (2005) 'Aquaporins in poplar: What a difference a symbiont makes!', *Planta*, 222(2), pp. 258–268. doi: 10.1007/s00425-005-1539-z.

Molina, R., Massicotte, H. B. and Trappe, J. M. (1992) 'Specificity phenomena in mycorrhizal symbioses: Community-ecological consequences and practical implications'. Available at:

https://www.researchgate.net/publication/239726751_Specificity_phenomena_in_mycorrhizal_symbioses_Community-ecological_consequences_and_practical_implications.

Muller, L. A. H., Vangronsveld, J. and Colpaert, J. V. (2007) 'Genetic structure of *Suillus luteus* populations in heavy metal polluted and nonpolluted habitats', *Molecular Ecology*, 16(22), pp. 4728–4737. doi: 10.1111/j.1365-294X.2007.03549.x.

- Navarro-Ródenas, A. *et al.* (2011) ‘Effect of water stress on in vitro mycelium cultures of two mycorrhizal desert truffles’, *Mycorrhiza*, 21(4), pp. 247–253. doi: 10.1007/s00572-010-0329-z.
- Naz, T. *et al.* (2023) ‘Industrially Important Fungal Carotenoids: Advancements in Biotechnological Production and Extraction’, *Journal of Fungi*, 9(5), p. 578. doi: 10.3390/jof9050578.
- Nehls, U. and Dietz, S. (2014) ‘Fungal aquaporins: cellular functions and ecophysiological perspectives’, *Applied Microbiology and Biotechnology*, 98(21), pp. 8835–8851. doi: 10.1007/s00253-014-6049-0.
- Ninni, L., Camargo, M. . and Meirelles, A. J. . (1999) ‘Water activity in poly(ethylene glycol) aqueous solutions’, *Thermochimica Acta*, 328(1–2), pp. 169–176. doi: 10.1016/S0040-6031(98)00638-8.
- Nordberg, H. *et al.* (2014) *The genome portal of the Department of Energy Joint Genome Institute: 2014 updates.*, *Nucleic Acids Res.* Available at: mycocosm.jgi.doe.gov/ (Accessed: 22 December 2023).
- Osmolovskaya, N. *et al.* (2018) ‘Methodology of drought stress research: Experimental setup and physiological characterization’, *International Journal of Molecular Sciences*, 19(12). doi: 10.3390/ijms19124089.
- Paradis, E. and Schliep, K. (2019) ‘ape 5.0: an environment for modern phylogenetics and evolutionary analyses in R’. *Bioinformatics*, pp. 526–528.
- Pérez-Moreno, J. *et al.* (2021) ‘Edible mycorrhizal fungi of the world: What is their role in forest sustainability, food security, biocultural conservation and climate change?’, *PLANTS, PEOPLE, PLANET*, 3(5), pp. 471–490. doi: 10.1002/ppp3.10199.
- Pettersson, N. *et al.* (2005) ‘Aquaporins in yeasts and filamentous fungi’, *Biology of the Cell*, 97(7), pp. 487–500. doi: 10.1042/BC20040144.
- Piwowarczyk, B., Kamińska, I. and Rybiński, W. (2014) ‘Influence of PEG generated osmotic stress on shoot regeneration and some biochemical parameters in Lathyrus culture’, *Czech Journal of Genetics and Plant Breeding*, 50(2), pp. 77–83. doi: 10.17221/110/2013-cjgpb.
- Querejeta, J., Egerton-Warburton, L. and Allen, M. (2003) ‘Direct nocturnal water transfer from oaks to their mycorrhizal symbionts during severe soil drying’, *Oecologia*, 134(1), pp. 55–64. doi: 10.1007/s00442-002-1078-2.
- R Core Team (2020) ‘R: A Language and Environment for Statistical Computing’. Vienna, Austria: R Foundation for Statistical Computing. Available at: <https://www.r-project.org/>.
- Rambaut, A. (2007) ‘FigTree’. Available at: <http://tree.bio.ed.ac.uk/software/figtree/>.
- Rozen, S. and Skaletsky, H. (no date) ‘Primer3’. Available at: <https://primer3.ut.ee/>.
- Ruytinx, J., Remans, T. and Colpaert, J. V (2016) ‘Gene expression studies in different genotypes of an ectomycorrhizal fungus require a high number of reliable reference genes’, *PeerJ Preprints*, 4:e2125v1. doi: 10.7287/peerj.preprints.2125v1.
- Schindelin, J. *et al.* (2012) ‘Fiji: an open-source platform for biological-image analysis’, *Nature Methods*, 9(7), pp. 676–682. doi: 10.1038/nmeth.2019.
- Smith, A. M. *et al.* (2010) *Plant Biology*. New York: Garland Science.
- Smith, S. E. and Read, D. J. (2008) ‘Structure and development of ectomycorrhizal roots’, in *Molecular Mycorrhizal Symbiosis*. Third. Wiley, pp. 47–61. doi: 10.1002/9781118951446.ch4.
- Spitzer, M. *et al.* (2014) ‘BoxPlotR: a web tool for generation of box plots’, *Nature Methods*, 11(2), pp. 121–122. doi: 10.1038/nmeth.2811.
- Spridille, T. *et al.* (2022) ‘Evolutionary biology of lichen symbioses’, *New Phytologist*, 234(5), pp. 1566–1582. doi: 10.1111/nph.18048.
- Studer, G. *et al.* (2020) ‘QMEANDisCo—distance constraints applied on model quality

estimation', *Bioinformatics*. Edited by A. Elofsson, 36(6), pp. 1765–1771. doi: 10.1093/bioinformatics/btz828.

Swedish forest industry significance (2016) *Swedish Forest Industries Federation*. Available at: <https://www.forestindustries.se/forest-industry/swedish-forest-industry/> (Accessed: 29 January 2024).

The Swedish Forest Industries Federation (2019) *The forest and sustainable forestry*. Available at: <https://www.swedishwood.com/wood-facts/about-wood/wood-and-sustainability/the-forest-and-sustainable-forestry/> (Accessed: 15 January 2024).

Trappe, J. M. (1977) 'Selection of Fungi for Ectomycorrhizal Inoculation in Nurseries', *Annual Review of Phytopathology*, 15(1), pp. 203–222. doi: 10.1146/annurev.py.15.090177.001223.

Vandesompele, J. *et al.* (2002) 'Accurate normalization of real-time quantitative RT-PCR data by geometric averaging of multiple internal control genes', *Genome Biology volume*, 3. doi: <https://doi.org/10.1186/gb-2002-3-7-research0034>.

Varma, A. (ed.) (2008) *Mycorrhiza*. Third. Berlin, Heidelberg: Springer Berlin Heidelberg. doi: 10.1007/978-3-540-78826-3.

Vasavada, N. (2016) *One-way ANOVA (ANalysis Of VAriance) with post-hoc Tukey HSD (Honestly Significant Difference) Test Calculator for comparing multiple treatments*.

Waterhouse, A. *et al.* (2018) 'SWISS-MODEL: homology modelling of protein structures and complexes', *Nucleic Acids Research*, 46(W1), pp. W296–W303. doi: 10.1093/nar/gky427.

van der Weele, C. M. *et al.* (2000) 'Growth of Arabidopsis thaliana seedlings under water deficit studied by control of water potential in nutrient-agar media', *Journal of Experimental Botany*, 51(350), pp. 1555–1562. doi: 10.1093/jexbot/51.350.1555.

Wu, Q.-S., Xia, R.-X. and Zou, Y.-N. (2008) 'Improved soil structure and citrus growth after inoculation with three arbuscular mycorrhizal fungi under drought stress', *European Journal of Soil Biology*, 44(1), pp. 122–128. doi: 10.1016/j.ejsobi.2007.10.001.

Xie, F. *et al.* (2012) 'miRDeepFinder: a miRNA analysis tool for deep sequencing of plant small RNAs', *Plant Molecular Biology*, 80(1), pp. 75–84. doi: 10.1007/s11103-012-9885-2.

Xie, F., Wang, J. and Zhang, B. (2023) 'RefFinder: a web-based tool for comprehensively analyzing and identifying reference genes', *Functional & Integrative Genomics*, 23(2), p. 125. doi: 10.1007/s10142-023-01055-7.

Xu, H., Cooke, J. E. K. and Zwiazek, J. J. (2013a) 'Phylogenetic analysis of fungal aquaporins provides insight into their possible role in water transport of mycorrhizal associations', *Botany*, 91(8), pp. 495–504. doi: 10.1139/cjb-2013-0041.

Xu, H. and Zwiazek, J. J. (2020) 'Fungal Aquaporins in Ectomycorrhizal Root Water Transport', *Frontiers in Plant Science*, 11(March), pp. 1–6. doi: 10.3389/fpls.2020.00302.

Yaniv, Z. and Werker, E. (1983) 'Absorption and secretion of polyethylene glycol by solanaceous plants', *Journal of Experimental Botany*, 34, pp. 1577–1584.

Yin, D. *et al.* (2018) 'Ectomycorrhizal fungus enhances drought tolerance of Pinus sylvestris var. mongolica seedlings and improves soil condition', *Journal of Forestry Research*. Springer Berlin Heidelberg, 29(6), pp. 1775–1788. doi: 10.1007/s11676-017-0583-4.

Yu, Z. and Fischer, R. (2019) 'Light sensing and responses in fungi', *Nature Reviews Microbiology*, 17(1), pp. 25–36. doi: 10.1038/s41579-018-0109-x.

Zardoya, R. (2012) 'Phylogeny and evolution of the major intrinsic protein family', *Biology of the Cell*, 97(6), pp. 397–414. doi: 10.1042/BC20040134.

Zhang, Y. *et al.* (2010) 'Improving drought tolerance of Casuarina equisetifolia seedlings by arbuscular mycorrhizas under glasshouse conditions', *New Forests*, 40(3), pp. 261–271. doi: 10.1007/s11056-010-9198-8.

Zhu, X., Song, F. and Xu, H. (2010) 'Influence of arbuscular mycorrhiza on lipid

peroxidation and antioxidant enzyme activity of maize plants under temperature stress', *Mycorrhiza*, 20(5), pp. 325–332. doi: 10.1007/s00572-009-0285-7.

Popular science summary

As the world grapples with climate change, one of its many challenges is the increasing occurrence of droughts, which are causing a significant rise in the death of tree seedlings after they are moved from nurseries to forests. It is more important than ever to develop forest management practices that can withstand these changes, to ensure our forests remain healthy and functional. A key player in this battle for resilience is a type of fungus known as ectomycorrhizal fungi (ECM). ECM fungi naturally live in symbiosis with trees such as pine and spruce and have been shown to aid the trees under conditions of drought. They can do this by, i.e., helping transport more water to the trees than the trees would otherwise be able to access. Aquaporin (AQP) proteins, vital for transporting water within the fungus and to the trees, play a key role in this process.

This master's thesis studied how three species of *Suillus*, a group of ECM fungi, react when subjected to drought. The study also explored the genes related to AQPs of these species. To simulate drought, the study used an approach involving an agar medium infused with varying concentrations of a substance called PEG-8000. The fungi showed unforeseen common trends in response to the drought simulation, such as changes in colouration and the density of their hyphae (the root-system of the fungi). However, the drought only resulted in significant differences in the overall size or weight of the fungi in one instance.

Furthermore, based on the DNA of the *Suillus*, the study explored the evolutionary relationship between different AQPs through what is called a phylogenetic analysis, as this has not been previously conducted in known literature. The analysis showed that the building blocks (amino acids) that make up the proteins of the AQPs in *Suillus* were largely consistent with those documented in existing research on fungal AQPs. A specific sequence of the amino acids called NPA was studied in detail, and notable distinctions were found in its pattern compared to the NPA sequences in other known AQPs. The study also made significant strides in setting up reliable reference genes for future research, which will help in studying how the expression of these fungi's genes behave under different levels of drought.

In essence, this research has laid a foundation for the understanding of drought resistance in a few species within the ECM fungal genus *Suillus*, which has facilitated future endeavours of understanding and optimising drought resistance of trees with ECM symbiotic relationships.

Acknowledgements

This research project was conducted in the autumn of 2023 at the Department of Forest Mycology and Plant Pathology at the Swedish University of Agricultural Sciences (SLU) and constitutes the master's thesis for the programme *Industrial and Environmental Biotechnology* at the KTH Royal Institute of Technology. I would like to express my immense gratitude to the many people who have helped me in my academic journey.

First and foremost, I extend my deepest gratitude to my main supervisor, Judith Lundberg-Felten. Her patience, expertise and thoughtful guidance have made this project not only educative but inspirational and fun. The time and effort she has invested in guiding me has been genuinely appreciated. Also, I want to thank my second supervisor Marisol Sanchez-Garcia for your assistance and advice which have greatly enriched my project.

I owe a great deal of thanks to my family for their constant support and encouragement, thank you for believing in me, always.

A special thanks Hampus Eskilsson for being a source of strength and motivation. Your confidence in my abilities has enhanced my academic and personal growth.

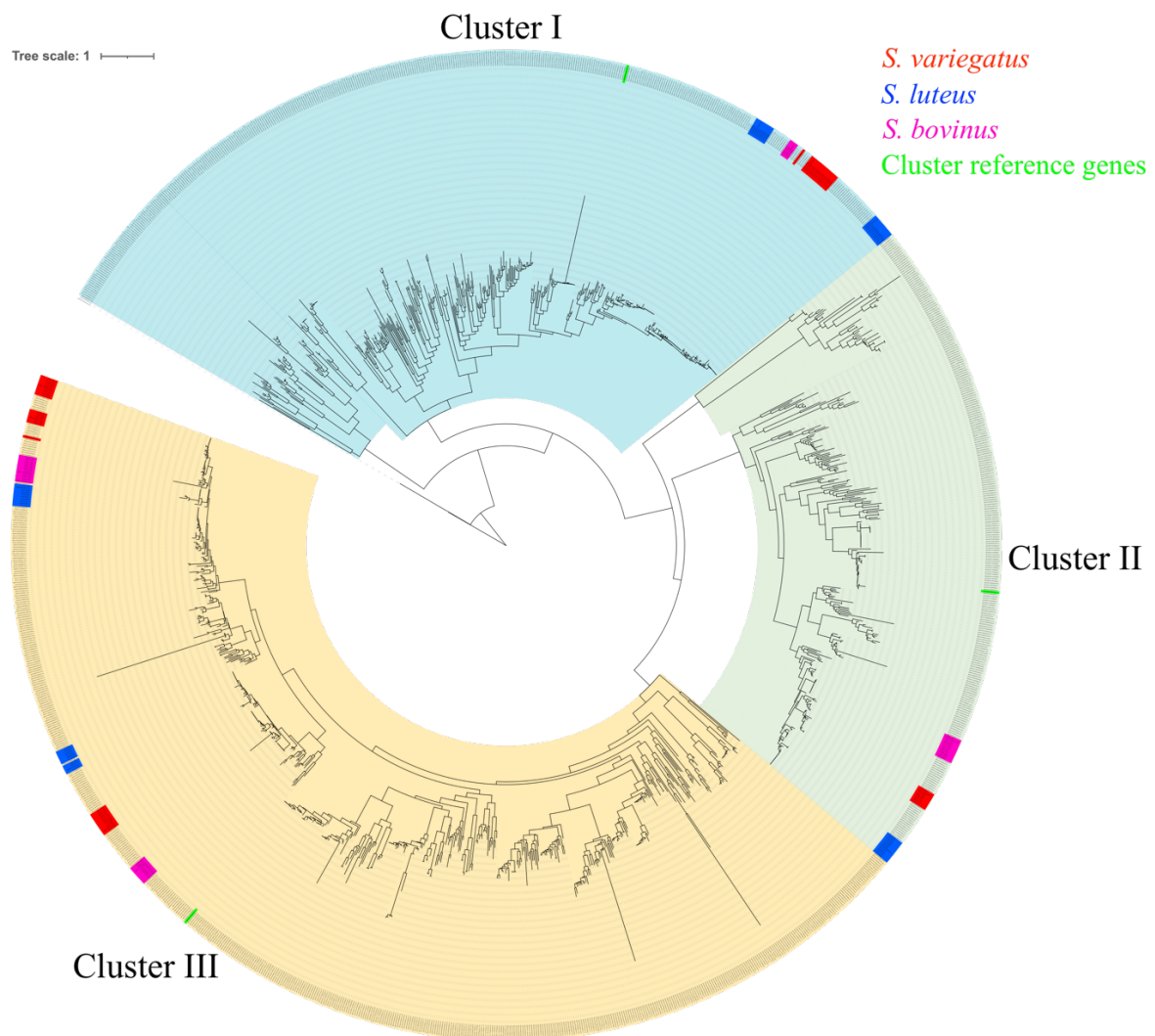
Furthermore, I would like to thank my examiner, Anders Dahlberg, Anna Berlin, the Director of Studies for the MSc education at SLU, and Per Berglund, the Program Director of the master's program in Industrial and Environmental Biotechnology at KTH, for their role in facilitating this unique research opportunity.

Lastly, I would like to extend my appreciation to the entire Department of Forest Mycology and Plant Pathology at the Swedish University of Agricultural Sciences for your warm welcome and help in the lab. In particular, I am indebted to Leslie Paul for his relentless assistance with all the technical challenges I faced.

Appendix

6.1 Appendix A – Phylogenetic tree of Dataset 1

Phylogenetic tree of three *Suillus* species from Dataset 1. Made with FigTree. The taxa of Cluster I are highlighted in blue, the taxa of Cluster II are highlighted in green, and the taxa of Cluster III are highlighted in yellow. Proteins from *S. variegatus* are written in red, proteins from *S. luteus* are written in blue, and proteins from *S. bovinus* are written in magenta. Three arrows are visible in the tree, each pointing at the reference proteins used to infer the clusters.



6.2 Appendix B – Sequence categorisation

As many of the 128 AQP sequences of the *Suillus* genus in dataset 2 (D2) were 100% identical on both protein- and transcript level. The sequences that were identical on both protein- and transcript level were grouped together according to Table 13, Table 14 and Table 15. The tables show the groups categorised according to cluster and species.

Table 13. Sequences in Cluster I grouped according to 100% identity on both protein- and transcript level.

Species	Group number	Sequence ID
<i>S. luteus</i>	1	jgi_Suilu4_2769856
		jgi_Suilu4_2916357
		jgi_Suilu4_2580063
		jgi_Suilu4_2580058
		jgi_Suilu4_2980430
		jgi_Suilu4_2769289
		jgi_Suilu4_2580136
		jgi_Suilu4_2820132
	2	jgi_Suilu4_2820131
		jgi_Suilu4_2906344
	3	jgi_Suilu4_2820113
		jgi_Suilu4_2769184
		jgi_Suilu4_2906337
		jgi_Suilu4_2837089
		jgi_Suilu4_2916343
		jgi_Suilu4_2980421
4	jgi_Suilu4_2770336	
	jgi_Suilu4_2820114	
	jgi_Suilu4_2820115	
	jgi_Suilu4_1802078	
<i>S. variegatus</i>	5	jgi_Suivar1_1553732
		jgi_Suivar1_1525994
		jgi_Suivar1_1470303
		jgi_Suivar1_1315224
		jgi_Suivar1_1343479
		jgi_Suivar1_1641565
		jgi_Suivar1_1534901
		jgi_Suivar1_1506244
		jgi_Suivar1_1506243
		jgi_Suivar1_1506242
		jgi_Suivar1_1482578
		jgi_Suivar1_1482580
		jgi_Suivar1_1482579
	jgi_Suivar1_1315373	
6	jgi_Suivar1_1293744	
<i>S. bovinus</i>	7	jgi_Suibov1_1107572
	8	jgi_Suibov1_1254846
	9	jgi_Suibov1_1242836

Table 14. Sequences in Cluster II grouped according to 100% identity on both protein- and transcript level.

Species	Group number	Sequence ID
<i>S. luteus</i>	1	jgi_Suilu4_2907192
		jgi_Suilu4_805694
		jgi_Suilu4_2771984
		jgi_Suilu4_2801031
		jgi_Suilu4_2822251
		jgi_Suilu4_2822250
		jgi_Suilu4_2838345
		jgi_Suilu4_2857184
		jgi_Suilu4_2917854
jgi_Suilu4_2981408		
<i>S. variegatus</i>	2	jgi_Suivar1_1358552
		jgi_Suivar1_1358553
	3	jgi_Suivar1_1358551
	4	jgi_Suivar1_1358554
	5	jgi_Suivar1_1582494
		jgi_Suivar1_1531614
	6	jgi_Suivar1_1340807
<i>S. bovinus</i>	7	jgi_Suibov1_1300379
		jgi_Suibov1_1238253
	8	jgi_Suibov1_1121825
		jgi_Suibov1_1077778
		jgi_Suibov1_1077988
		jgi_Suibov1_1199461
		jgi_Suibov1_1220003
		jgi_Suibov1_1199460
		jgi_Suibov1_1121823
		jgi_Suibov1_1220002

Table 15. Sequences in Cluster III grouped according to 100% identity on both protein- and transcript level.

Species	Group number	Sequence ID
<i>S. luteus</i>	1	jgi_Suilu4_1739277
		jgi_Suilu4_2777018
	2	jgi_Suilu4_2825494
		jgi_Suilu4_2982784
		jgi_Suilu4_2908359
		jgi_Suilu4_2804280
		jgi_Suilu4_2825491
		jgi_Suilu4_2825490
	3	jgi_Suilu4_2804279
		jgi_Suilu4_2139653
		jgi_Suilu4_2139720
	4	jgi_Suilu4_2139284
		jgi_Suilu4_2139236
		jgi_Suilu4_2140581
		jgi_Suilu4_2139929
		jgi_Suilu4_2919567
jgi_Suilu4_2839772		
<i>S. variegatus</i>	5	jgi_Suilu4_2860740
		jgi_Suilu4_2140422
		jgi_Suivar1_1418285
		jgi_Suivar1_1491563
		jgi_Suivar1_1515135
		jgi_Suivar1_1491565
		jgi_Suivar1_99852
	6	jgi_Suivar1_1542096
		jgi_Suivar1_1528761
	7	jgi_Suivar1_1515134
		jgi_Suivar1_1491564
	8	jgi_Suivar1_1646105
		jgi_Suivar1_1473559
	9	jgi_Suivar1_99286
jgi_Suivar1_1349285		
10	jgi_Suivar1_1542095	
	jgi_Suivar1_99436	
11	jgi_Suivar1_1553710	
	jgi_Suivar1_1343453	
	jgi_Suivar1_1641543	
12	jgi_Suivar1_263584	
	jgi_Suivar1_1534877	
13	jgi_Suivar1_1482539	
	jgi_Suivar1_263491	
14	jgi_Suivar1_1525983	
	jgi_Suivar1_1293483	
<i>S. bovinus</i>	15	jgi_Suivar1_1274156
		jgi_Suibov1_1128832
	16	jgi_Suibov1_1128833
		jgi_Suibov1_1128831
	17	jgi_Suibov1_1239066
jgi_Suibov1_1101685		

	jgi_Suibov1_1080079
18	jgi_Suibov1_1247553
19	jgi_Suibov1_60087
	jgi_Suibov1_1128808
	jgi_Suibov1_1128815
	jgi_Suibov1_1128811
20	jgi_Suibov1_1128810
	jgi_Suibov1_1128807
	jgi_Suibov1_1128814
	jgi_Suibov1_1128812
21	jgi_Suibov1_1101681
22	jgi_Suibov1_60802
